Inverse electron demand Diels-Alder pyridazine elimination: synthetic tools for chemical immunology

Geus, M.A.R. de

4

Chemical control over T-cell activation *in vivo*: design and synthesis of *trans*-cyclooctene-modified MHC-I epitopes

Parts of this chapter were published as:
A. M. F. van der Gracht, M. A. R. de Geus, M. G. M. Camps, T. J. Ruckwardt, A. J. C. Sarris, J. Bremmers, E. Maurits, J. B. Pawlak, M. M. Posthoorn, K. M. Bonger, D. V Filippov, H. S. Overkleeft, M. S. Robillard, F. Ossendorp, S. I. van Kasteren, *ACS Chem. Biol.* **2018**, *13*, 1569–1576.

4.1 Introduction

Cell-to-cell contact is one of the essential means of information transfer in metazoans. Few examples of such cell-cell contacts result in more drastic phenotypic changes than those between cytotoxic T-lymphocytes (CTLs) and antigen presenting cells (APCs).[1] Naïve T-cells leave the thymus as small, featureless cells with minimal metabolism, but with a strong lymph node homing capacity, reliant on L-selectin (CD62L) and various integrins.[2] Each cell has a specific T-cell receptor (TCR) capable of recognizing a

peptide presented by an APC on a major histocompatibility type-1 complex (MHC-I).[1] Upon recognition of its cognate peptide-MHC-I (pMHC), in combination with co-stimulatory signals co-presented by the APC, massive and rapid phenotypic changes will transform the naïve CTL into a cell capable of killing any non-APCs displaying this cognate peptide on their MHC-I.[3] This is one of the major mechanisms by which tumors and virus-infected cells are routinely cleared from the body and harnessing these traits underpins many of the cancer immunotherapies targeted to tumor neo-epitopes.[4]

Antigen presentation is an important prerequisite for T-cell activation. Nucleated cells proteolytically degrade endogenous proteins into small peptides, which can enter the endoplasmic reticulum (ER) via the transporter associated with antigen processing (TAP), followed by loading on MHC-I, passage to the cell surface via the Golgi system and presentation to $CD8^+$ T-cells (CTLs).[3,5] Exogenously derived polypeptides are normally presented on MHC-II complexes to $CD4^+$ T-cells (helper T-cells) via a different pathway by professional APCs (dendritic cells (DCs), macrophages and B-cells). Here, the MHC class II compartment (MIIC) facilitates deconstruction of the invariant chain (Ii) of MHC-II and ultimately allows binding of a peptide degraded in endosomes.[5] However, antigen cross-presentation[6] allows DCs to process exogenous polypeptides towards MHC-I presentation. It is not clear for this process whether and to which extent antigen processing occurs in the cytosol via proteasomes (cytosolic pathway) or in endocytic compartments via cathepsins (vacuolar pathway).[6]

The binding of the TCR is sensitive. As few as one copy of a cognate peptide can instigate the signaling cascade *in vitro*.[7,8] It is also selective, as this recognition takes place in the context of 10,000s of copies of non-cognate peptides on the same APC.[9,10] Even single amino acid substitutions are capable of curtailing,[11] or even abolishing T-cell activation.[12–14] A factor that complicates T-cell activation studies further is that there is no correlation between the binding strength *in vitro* and the strength of TCR-signaling that follows activation.[15] Less is known about the *in vivo* activation of T-cells.[16] The contacts between T-cells and APCs are, for example, more transient and dynamic in nature compared to those found *in vitro*.[17–20] The lack of a defined starting point to these contacts complicates the study of T-cell activation kinetics, and methods allowing the study of early T-cell activation events with real-time control over activation *in vivo* are needed to study these processes.[16]

Control over T-cell activation using protecting group strategies to achieve temporal control *in vitro* is an emerging field. Two approaches have been reported in which the ε-amines of lysine residues within either a helper T-cell epitope[21,22] or a cytotoxic T-cell epitope[14] are blocked with a protecting group (Figure 1). These caged epitopes are

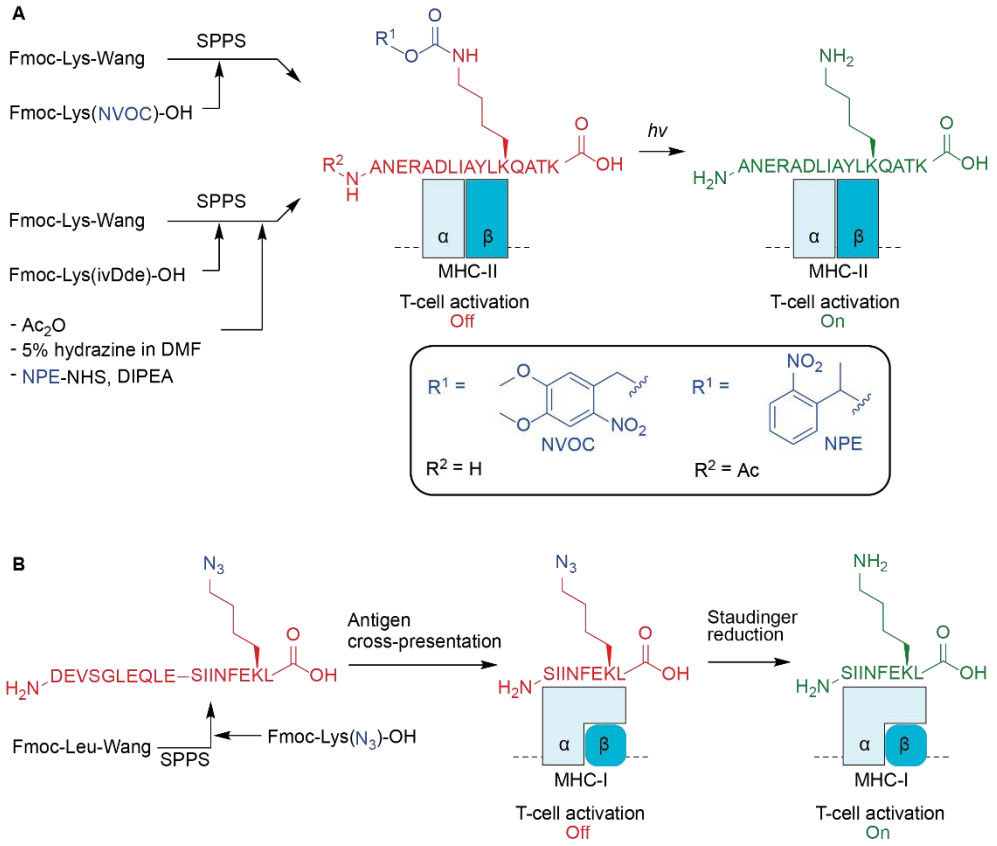

Figure 1 Previously reported *in vitro* approaches to achieve temporal control over T-cell activation, including SPPS strategies to obtain the caged antigens. A) Photodecaging strategy to gain control over helper T-cell ($CD4^+$) activation. MHC II epitope MCC88-103 (moth cytochrome c) was protected on Lys99 using NVOC (6-nitroveratryloxycarbonyl) or NPE (1-ortho-nitrophenyl-ethyl urethane) photocages by DeMond *et al.*[21] and Huse *et al.*,[22] respectively. B) Chemodecaging strategy to study antigen cross-presentation and subsequent cytotoxic T-cell ($CD8^+$) activation reported by Pawlak *et al.*[14] MHC I epitope OVA257-264 (ovalbumin) was protected on Lys263 using an azide which could be deprotected *in vitro* by Staudinger reduction.

accessible either by directly incorporating modified Fmoc-lysine building blocks[14,21] or by utilizing selective sidechain modifications[22] during solid phase peptide synthesis (SPPS). Addition of a deprotection reagent, such as UV-light to remove NVOC (6-nitroveratryloxycarbonyl) or NPE (1-ortho-nitrophenyl-ethyl urethane) groups,[21,22] or water-soluble phosphines to reduce azides to amines,[14,23] provided this temporal control in the petri dish.

Arguably, the use of (UV) light as a trigger to activate T-cell epitopes has intrinsic limitations: poor tissue penetration even at higher wavelengths essentially prohibits systemic application of photocaged T-cell epitopes. On paper, bioorthogonal chemistry

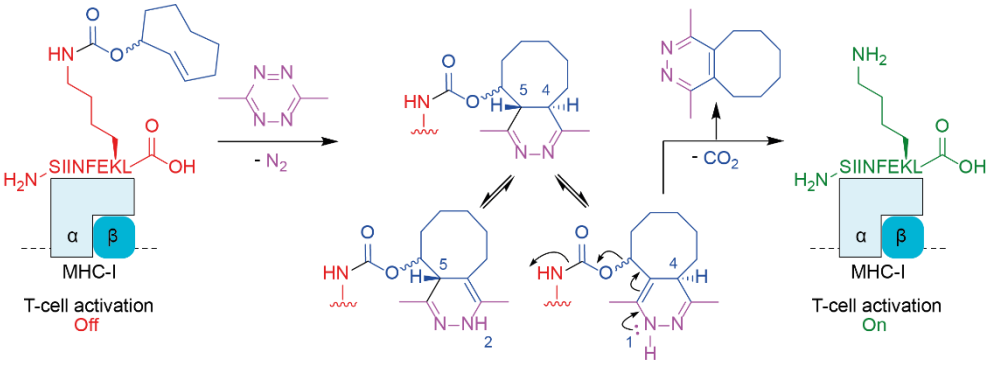

Figure 2 Design of caged peptides for *in vivo* control over T-cell activation. Inverse electron-demand Diels Alder (IEDDA) pyridazine elimination between a silent *trans*-cyclooctene-modified epitope and a tetrazine liberates antigenicity of the peptide. Initial [4+2] cycloaddition, tautomerization and elimination results in the free lysine ε-amine upon which a T-cell can recognize the epitope again and become activated.

has no such tissue-penetrating limits, however the chemistry needs to be effective (more so than the previously reported Staudinger reduction)[14] and all reagents able to penetrate all tissues. In this respect, the most versatile bioorthogonal chemistry developed to date for *in vivo* applications in terms of yield, speed and side reactions comprises the inverse electron demand Diels-Alder reaction (IEDDA).[24] This [4+2] cycloaddition reaction occurs between an electron-poor diene (normally an *s*-tetrazine) and an electron-rich dienophile (most often a strained alkene). The tetrazine ligation between a tetrazine and a *trans*-cyclooctene, was initially reported as an ultra-fast bioorthogonal ligation reaction by the Fox group.[25]

Recently, the IEDDA reaction was redesigned to serve as a bioorthogonal deprotection reaction.[26] In this variant of the IEDDA, the 4,5-dihydropyridazine, resulting from [4+2] cycloaddition of a tetrazine and a *trans*-cyclooctene (TCO) bearing a carbamate at the allylic position, tautomerizes to 1,4- and 2,5-dihydropyridazines. The 1,4-tautomer can then undergo elimination of a carbamate-linked biomolecule at the allylic position, resulting in the liberated biomolecule and CO_2 (Figure 2). Mechanistic investigations concerning this IEDDA pyridazine elimination reaction are currently a field of interest,[27–29] and *in vivo* applications have frequently been reported.[30–36]

This Chapter presents the design and synthesis of TCO modified MHC-I epitopes, resulting in a new method based on the IEDDA pyridazine elimination to provide chemical control over the activation of T-cells (Figure 2). The TCO protecting group was optimized for solubility and on-cell deprotection yield. This novel approach is generic based on the effectiveness for two separate epitopes and works with different T-cells *in vitro*, as well as *in vivo*.

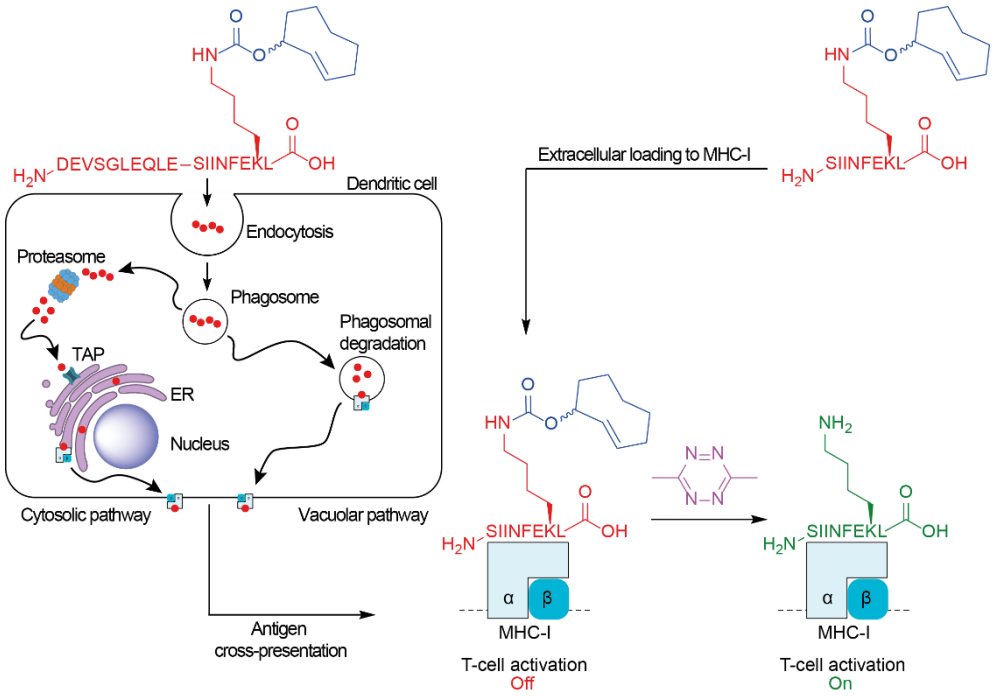

Figure 3 Rationale for TCO carbamate modification of minimal epitopes and extended peptide sequences. Minimal epitopes enable direct, extracellular loading on MHC-I, whereas an extended peptide sequence containing the epitope is initially endocytosed by DCs, followed by antigen cross-presentation via the cytosolic and/or vacuolar pathway.

4.2 Results and discussion

To determine whether IEDDA pyridazine elimination was amenable for *in vivo* T-cell activation and to compare its efficacy with that of the previously reported strategy based on Staudinger reduction,[14] $OVA_{257-264}$ (OT-I, SIINFEKL) was selected as model epitope. The crucial lysine ε-amino group within this epitope is amenable for chemical modification, thereby disabling T-cell activation without disrupting MHC-I binding affinity.[14,37] It was therefore envisioned that TCO carbamate modification of this position would result in silenced MHC-I epitopes. Modification of the minimal epitope results in a probe for direct, extracellular loading on MHC-I complexes, whereas modification of an extended peptide sequence results in a silenced epitope which is initially subjected to antigen cross-presentation (Figure 3).

A direct Fmoc SPPS based synthetic strategy, featuring a lysine building block with TCO carbamate modification, was explored in Chapter 3 without adequate results. Therefore, a synthetic strategy was devised where the TCO carbamate moiety could be installed under solution phase conditions. Cyclooctene N-hydroxysuccinimide (NHS)

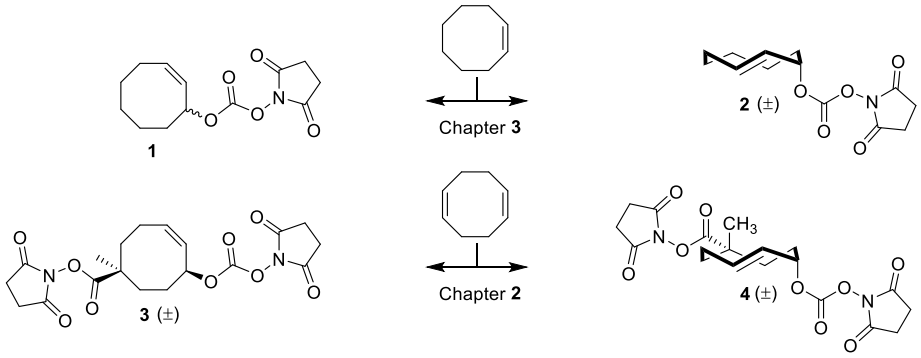

Scheme 1 CCO and TCO NHS-carbonates **1 – 4** employed in this Chapter for regioselective installation of cyclooctene carbamate moieties on lysine ε-amino groups.

carbonates **1** – **2** (Chapter 3) and bifunctional cyclooctene NHS carbonates **3** – **4** (Chapter 2) were selected as appropriate reagents for chemoselective introduction of cyclooctenes on peptide scaffolds containing a lysine ε-amino group (Scheme 1). An important requisite for these reagents was the absence of other reactive amine groups during the conjugation reaction.

The peptide sequence $OVA_{257-264}$ (SIINFEKL) was synthesized using standard Fmoc SPPS conditions followed by N-terminal protection with the methylsulfonylethyloxycarbonyl (MSc) group[38] to improve the solubility of the liberated peptide after acidic cleavage (TFA/H_2O/TIPS; 95:2.5:2.5 *v/v*) from the resin and to enable selective modification of the lysine ε-amine in the subsequent step (Scheme 2). From the HPLC-purified intermediate (MSc-SIINFEKL, **5**) CCO- and (axial) TCO carbamate derivatives of SIINFEKL were synthesized by reaction with NHS carbonates **1** and **2** followed by deprotection under basic conditions of the MSc group to provide the *cis*- and *trans*-cyclooctene protected SIINFEKL-derivatives **6** and **7**. Peptide **5** was also reacted with the NHS-carbonates of reagents **3** and **4** in the presence of their sterically hindered NHS-esters. Next, the latter were reacted with ethanolamine to install an extra polar moiety on the ring systems. This resulted in the more water-soluble caged SIINFEKL derivatives **8** and **9** after MSc deprotection. The first two steps of this sequence, selective NHS carbonate coupling followed by NHS ester reaction, were compatible in a one-pot procedure guided by LC-MS monitoring. Caged peptides **6** – **9** were obtained in 10 – 20% yield over 3 steps after HPLC purification.

An N-terminally extended peptide sequence, $OVA_{247-264}$ (DEVSGLEQLESIINFEKL), was synthesized with bifunctional TCO modification (Scheme 3A). This extended peptide sequence still contains only one lysine residue and no other competing sidechains (e.g. cysteine). Therefore, the MSc-protected peptide **10** could be selectively modified with

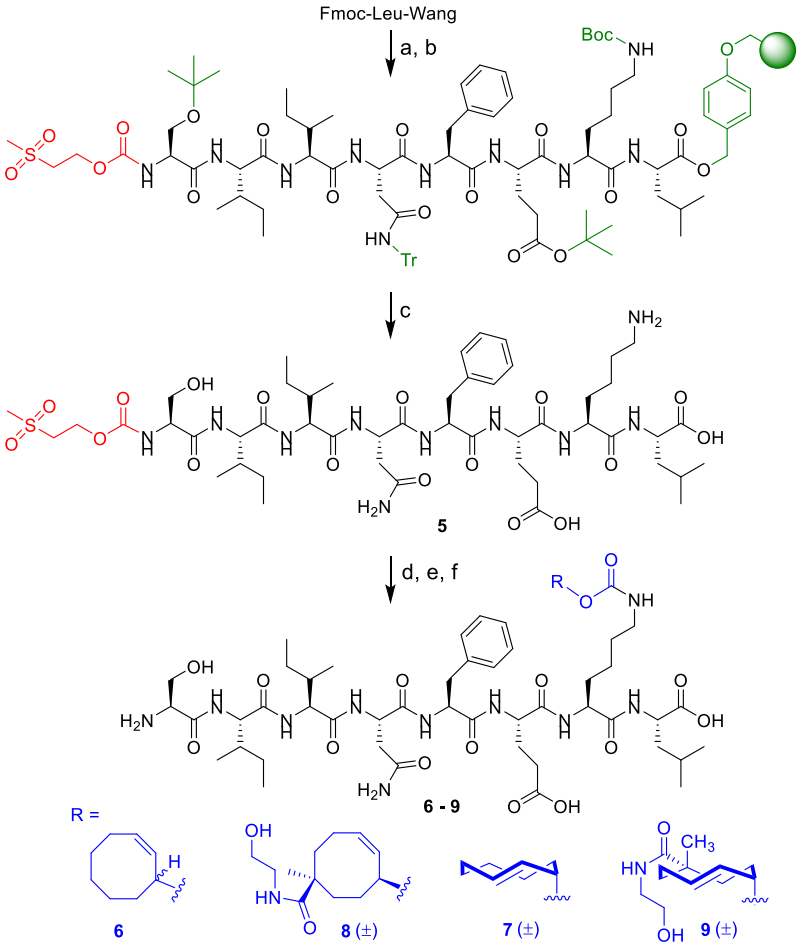

Scheme 2 Synthesis of caged peptides **6** – **9**. Reagents/conditions: (a) Fmoc SPPS from Fmoc-Leu-Wang; (b) MSc-OSu (**23**), DIPEA, NMP, rt; (c) TFA / H_2O / TIPS (95:2.5:2.5), rt, 23%; (d) NHS-CCO (**1**), NHS-TCO (**2**), NHS-bCCO (**3**) or NHS-bTCO (**4**), DIPEA, DMF, rt; (e) ethanolamine, DMF, rt; (f) dioxane/MeOH/4 M NaOH (7.5:2.25:0.25), rt, 16% (**6**), 20% (**7**), 19% (**8**), 14% (**9**) over three steps.

the TCO moiety using the established methodology after switching from DMF to DMSO as solvent for the NHS-coupling reactions. Peptide **11** was obtained in 41% yield over 3 steps after HPLC purification.

To assess whether the uncaging approach could be used for other key lysine residues as well as other MHC-I haplotype ligands, a second epitope in which T-cell recognition is dependent on a critical lysine was selected, namely the $D^bM_{187\text{-}195}$ peptide (NAITNAKII) from respiratory syncytial virus (RSV).[39–41] This nonamer sequence binds MHC-I haplotype D^b and the recognition by T-cells is critically dependent on Lys-

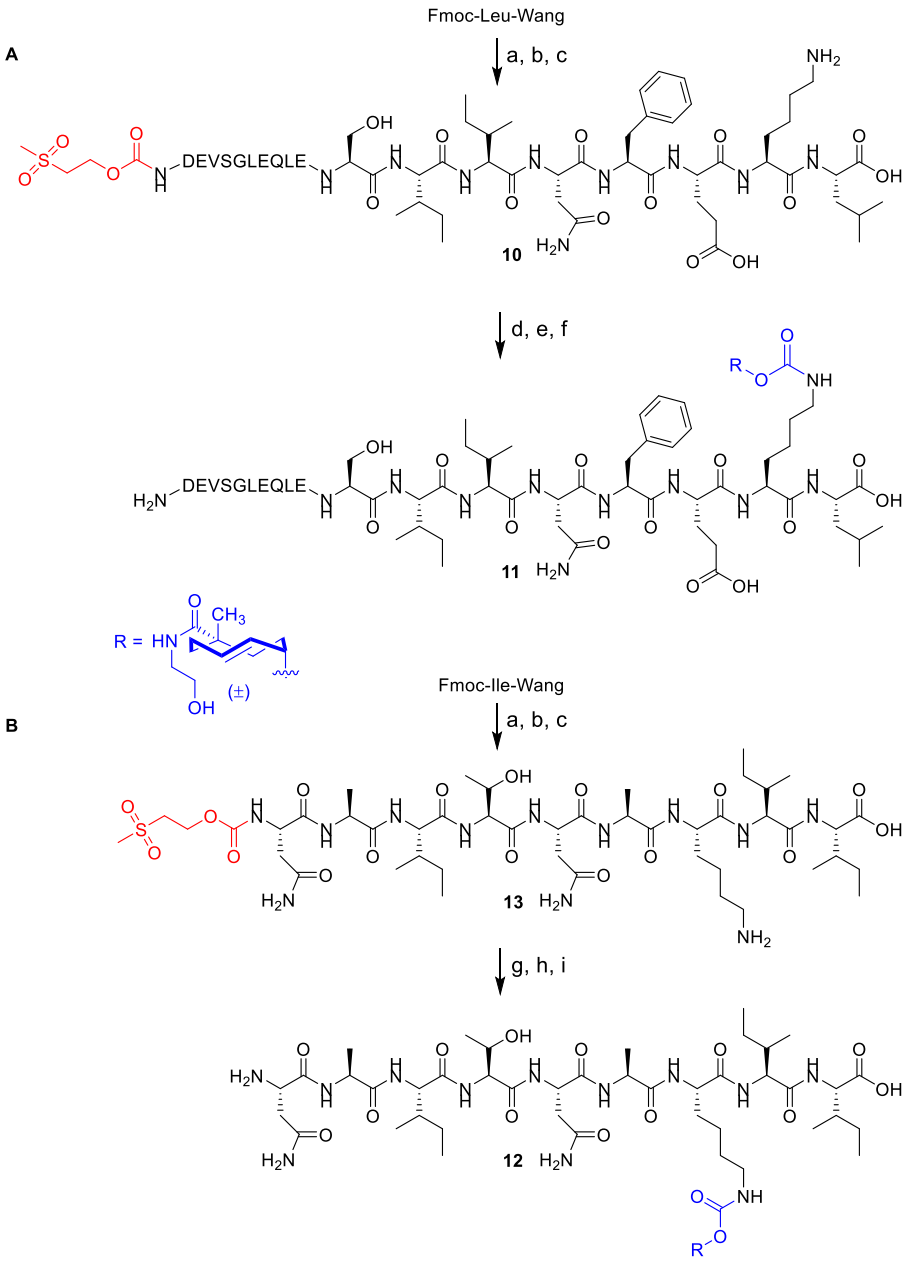

Scheme 3 Synthesis of caged peptides **11** and **12**. Reagents/conditions: (a) Fmoc SPPS from Fmoc-Leu-Wang (A) and Fmoc-Ile-Wang (B); (b) MSc-OSu (**23**), DIPEA, NMP, rt; (c) TFA / H_2O / TIPS (95:2.5:2.5), rt, 14% (**10**), 16% (**13**); (d) NHS-bTCO (**4**), DIPEA, DMSO, rt; (e) ethanolamine, DMSO, rt; (f) dioxane/MeOH/4 M NaOH (7.5:2.25:0.25), rt, 41% over three steps; (g) NHS-bTCO (**4**), DIPEA, DMF, rt; (h) ethanolamine, DMF, rt; (i) dioxane/MeOH/4 M NaOH (7.5:2.25:0.25), rt, 13% over three steps.

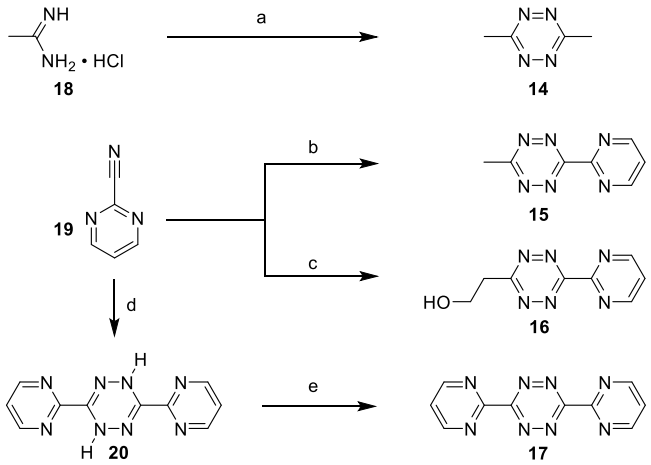

Scheme 4 Synthesis of tetrazines **14** - **17**. Reagents/conditions: (a) i. hydrazine hydrate, H_2O, rt; ii. HNO_3/H_2O, Cu, 0°C, 18% over two steps; (b) i. MeCN, $Zn(OTf)_2$, hydrazine hydrate, 60°C; ii. HNO_3/H_2O, Cu, 0°C, 31% over two steps; (c) i. 3-hydroxypropanenitrile, $Zn(OTf)_2$, hydrazine hydrate, 60°C; ii. $NaNO_2$, HCl, rt, 3% over two steps; (d) THF, HCl, hydrazine hydrate, reflux; (e) DMF, HNO_3/H_2O, Cu, rt, 14% over two steps.

193 recognition,[42] which has previously been subjected to caging.[14] The synthesis of a bifunctional TCO caged variant of this peptide (**12**) was accomplished from the MSc-protected intermediate (**13**) using the previously described method (Scheme 3B).

A panel of tetrazines (**14 – 17**) was synthesized to serve as deprotection agents for the caged peptides (Scheme 4). Cyclization of acetamidine hydrochloride (**18**) and hydrazine monohydrate under aqueous conditions was followed by direct oxidation with NO_2 (g), which was generated externally by adding HNO_3 to Cu, to afford 3,6-dimethyltetrazine (**14**)[26] in 18% yield. Condensation of **19**, MeCN and hydrazine hydrate in the presence of $Zn(OTf)_2$ afforded **15**[27] after oxidation with NO_2 (g) in 31% yield. While the initial cyclization step worked similarly for the synthesis of **16**[27], the oxidation step with NO_2 (g) primarily led to decomposition of the product. Instead, oxidation was achieved by slowly acidifying the crude reaction mixture with HCl after adding $NaNO_2$. Chromatographic purification was followed by recrystallization in EtOAc to obtain **16**.[27] Dihydrotetrazine **20** was isolated by extraction after cyclization of **19** and hydrazine hydrate under reflux conditions. Oxidation of **20** with NO_2 (g) in DMF led to the formation of a purple precipitate, which was filtered and recrystallized in $CHCl_3$ to obtain **17**.[43]

Immunological experiments summarized in this Chapter were performed by A.M.F. van der Gracht (Leiden University), N.A.M. Ligthart (Leiden University), M.G.M. Camps (Leiden University Medical Center) and T.J. Ruckwardt (NIH, USA). Full details can be found in the recently published article[44] *and PhD thesis (A.M.F. van der Gracht).*

The binding of peptides **6 – 9** to MHC-I (H2-K^b) was examined using TAP deficient RMA-S cells.[45,46] TCO modification of the SIINFEKL epitope on the Lys ε-amine did not impair MHC-I binding. The T-cell hybridoma B3Z,[47] which is specific for $OVA_{257-264}$ (SIINFEKL), was also not activated by **6 - 9** when presented on dendritic cells.

Caged epitopes **6 - 9** were loaded on dendritic cells (DC2.4 cells)[48] and incubated with 50 μM of 3,6-dimethyl-tetrazine (**14**) for 30 minutes. T-cell proliferation was measured after 17 hours as beta-galactosidase-directed CPRG (chlorophenol red-β-D-galactopyranoside) hydrolysis, which is in direct correlation with IL-2 promotor activity, due to its inclusion under the NFAT-promotor in the B3Z T-cell line.[47] No T-cell response was observed for the tetrazine-unreactive peptides **6** and **8**. However, tetrazine-reactive peptides **7** and **9** gave 42% ± 4.2% and 82% ± 4.4% of the response observed for the wild type epitope, respectively. The stability of the TCO-moiety for peptides **7** and **9** was determined in full medium and FCS (fetal calf serum), revealing poor solubility for **7** and stability up to 4 hours in FCS for **9** (Figure S1). Caged epitope **9** was selected for further experiments due to superior uncaging yield, ease of purification and enhanced solubility.

The speed of uncaging of peptide **9** was investigated using the recently reported asymmetric tetrazines by Fan *et al*.,[27] which were shown to have improved kinetics due to the combination of an electron withdrawing group (EWG) and a small, electron donating group (EDG) as substituents on the tetrazine ring (Figure 4A). 3-Methyl-6-pyrimidinyl-tetrazine (**15**) and 3-hydroxyethyl-6-pyrimidinyl-tetrazine (**16**) indeed showed improved uncaging rates and efficacy (Figure 4B-C) compared to **14** (two EDGs), with maximal T-cell activation already observed at the first (1 min) time point, while for **14** the maximal T-cell activation is reached at 30 min incubation. Conversely, 3,6-dipyrimidinyl-tetrazine (**17**) (two EWGs) showed no detectable elimination. Qualitative LC-MS confirmed these findings, including the formation of a stable IEDDA ligation product for **17**. These results are also in agreement with the hypothesis that EWGs accelerate the [4+2] cycloaddition step and suppress subsequent elimination, whereas small, EDGs are essential for the elimination reaction.[27] Tetrazine **17** therefore broadens the scope of the method presented in this Chapter: the substituents of the tetrazine employed dictate whether T-cell activation is switched on (Figure 2) or remains off (Figure 4D). The previously reported dextran-functionalized tetrazine (**21**), which has reduced yield and uncaging speed compared to **14** *in vitro*, but performs

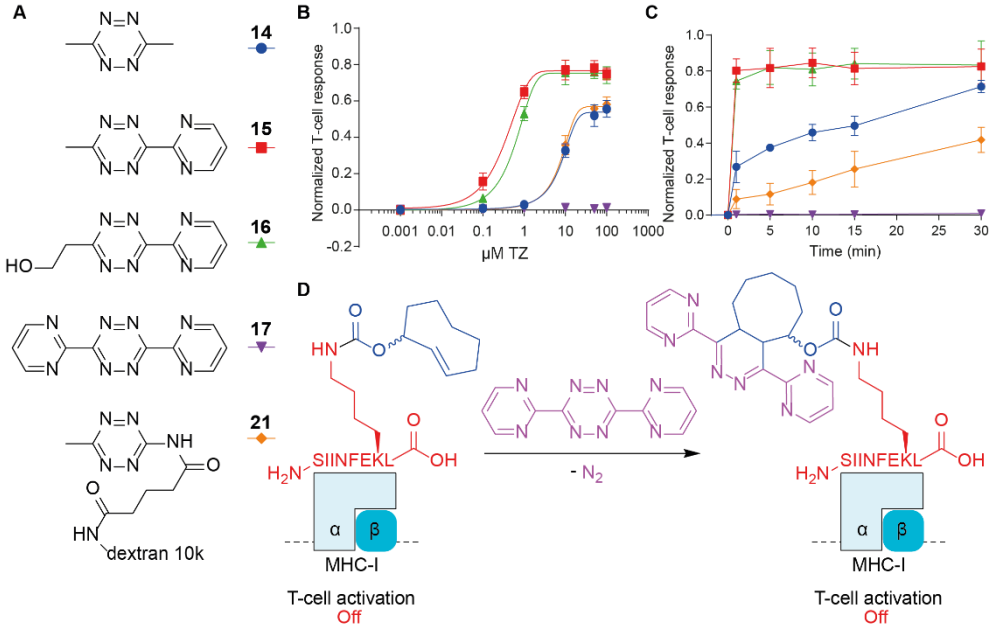

Figure 4 *In-vitro* kinetics of uncaging of peptide **9** using different tetrazines. A) Structures of tetrazines **14** – **17** and **21**. B/C) Deprotection of 100 nM **9** using DC2.4 cells as APCs and B3Z cells as T-cells. T-cell activation was compared to wild-type response (SIINFEKL; set at 1.0 normalized T-cell response) by measuring absorption (AU) of beta-galactosidase-directed CPRG hydrolysis after 17 hours. All experiments have been done twice in triplicate, error bars represent the standard deviation. Experiments were performed by A.M.F. van der Gracht (Leiden University). Tetrazine **21** was provided by Tagworks Pharmaceuticals. B) Uncaging of **9** with tetrazines **14** – **17** and **21** for 30 minutes at the indicated concentrations. C) Deprotection reaction of **9** with tetrazines **14** – **17** and **21** at 10 μM of tetrazine at increasing incubation times. Tetrazine **17** blocks T-cell activation and tetrazine **15** and **16** show improved uncaging speed compared to tetrazine **14**. Tetrazine **21** shows reduced uncaging speed and increases linear. Relative T-cell response is normalized between SIINFEKL 100 nM response as 1.0 and no peptide background signal 0.0. D) Tetrazine **17** broadens the scope of the method presented in this Chapter: the substituents of the tetrazine employed dictate whether T-cell activation is switched on (Figure 2) or remains off.

better *in vivo* due to reduced clearance,[30,49] was also evaluated in the *in vitro* assay (Figure 4A-C). Tetrazine **21** showed similar concentration dependent behavior as **14**, but slower uncaging speed although linear in time.

Stability, clearance and toxicity are other important criteria for the selection of tetrazines towards *in vivo* experiments. Stability in FCS was determined for tetrazines **14 – 17**; **17** is very unstable in serum while **14** showed no degradation. After 24 hours, 25% of **15** and 40% of **16** were still intact (Figure S2). Tetrazine **14** has been reported to be nontoxic *in vivo* up to 140 mg/kg (1.25 mmol/kg) in mice.[32] Tetrazines **14**, **16**

and **21** were selected for further experiments, which also showed negligible toxicity on APCs.

OT-I-mice, which have a homogeneous T-cell population selective for the SIINFEKL-epitope,[50] were used for *in vivo* experiments. Carboxyfluorescein succinimidyl ester (CFSE)-labeled OT-I T-cells[50] were adoptively transferred in recipient C57BL/6 mice on day -1. On day 0 the mice were either injected with peptide **9** or SIINFEKL in the tail base. After 3 days, the amount of T-cell proliferation was assessed by flow cytometry through CFSE-dilution.[51] Under these conditions, compound **9** induced very low levels of proliferation of OT-I CTLs and upon injection with tetrazine **14**, CTL proliferation was induced similarly compared to SIINFEKL (3.1% ± 0.11% vs 4.4 % ± 0.05 % divided OT-I of total lymphocytes).

Decaging of **12** with **14** (50 μM) in a mixed splenocyte assay, using (CFSE)-labeled T-cells with a specific TCR for NAITNAKII, showed the same level of control over T-cell activation as seen for SIINFEKL/OT-I, suggesting application to lysine-cognate TCRs in general.

Antigen cross-presentation of peptide **11** was studied using D1 dendritic cells and B3Z T-cells. Current results indicate **11** is cross-presented at a lower rate compared to the native peptide sequence. Furthermore, TCO-modification may alter cross presentation pathways, as the effects of inhibitors for the cytosolic and vacuolar pathways were also different. One difficulty with these studies is the persistence of presentation by D1 cells after tetrazine treatment. Additionally, if the tetrazine has adequate membrane permeability to enter D1 cells, intracellular decaging would lead to an overestimation of cross-presentation. Fixation of APCs improved reliability of current results and the development of tetrazines with intra- or extracellular targeting moieties are of importance for further experiments.

4.3 Conclusions

A new method, based on the IEDDA pyridazine elimination,[26] that allows chemical control over T-cell activation *in vitro* and *in vivo* is reported. MHC-I epitopes were synthesized using Fmoc SPPS, followed by N-terminal protection with the base-labile MSc-protecting group[38] and acidic cleavage from the resin. The desired lysine ε-amino group could then be regioselectively protected as a TCO carbamate in solution, followed by MSc deprotection under basic conditions and HPLC purification of the TCO-modified peptide. In the absence of a tetrazine, the lysine-caged epitopes show no T-cell receptor activation while MHC-I binding was not affected. Upon deprotection, T-cell receptor activation was restored. The lysine cage was implemented in two different epitopes, suggesting a generic application to lysine-sensitive TCRs.

In vivo results showed very similar T-cell proliferation potency upon decaging epitope **9** compared to the natural epitope, whereas the caged epitope showed no proliferation by itself. By combining this uncaging technique with injectable tetrazine-hydrogels[33] or antibody-epitope conjugates,[30] the activation of T-cells could even be controlled more precisely in future experiments. This can provide new angles to the study of CTL-activation *in vivo,* analogous to that which has been achieved *in vitro* using photo-[21,22,52] and chemo[14]-deprotection.

The caged epitope approach was also applied to study antigen cross-presentation. Preliminary experiments suggest that TCO-modification may alter cross-presentation pathways. One major difficulty in these experiments is to separate intra- and extracellular decaging. Current efforts are aimed towards this challenge.

4.4 Supporting figures

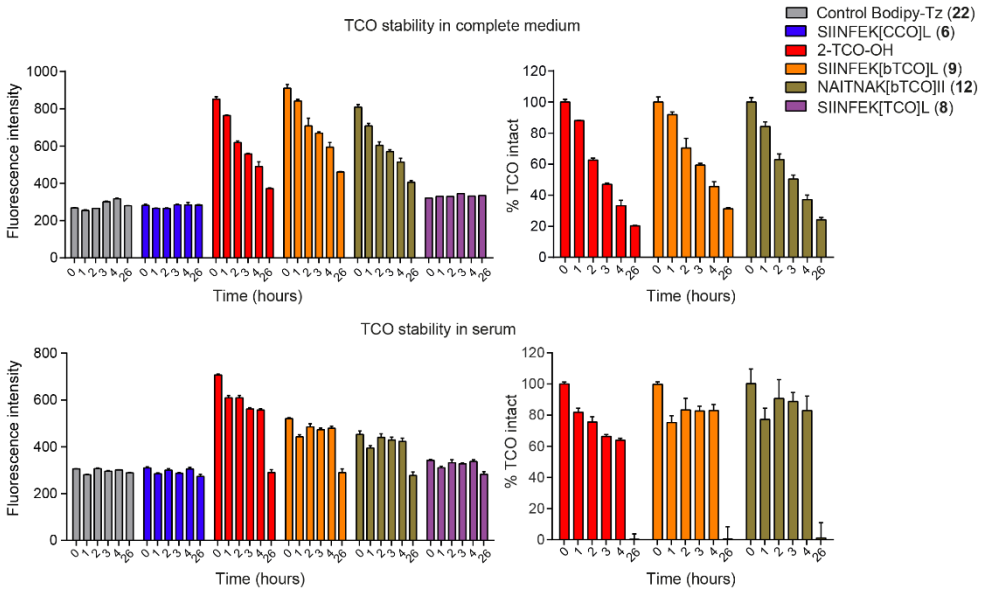

Figure S1 TCO stability in complete medium and serum. Stability of TCO constructs were determined by incubation in the desired solvent (PBS, Full Medium or Fetal Calf Serum) at 37°C over a time period of 24 h. After incubation the compounds were co-incubated with Bodipy-Tz (**22**) and fluorescence intensity was measured directly. The bar charts represent the fluorescent intensity of the samples after 50 min incubation with **22**, from which the % intact TCO was determined compared to 0 h incubation in solvent. Formula after baseline correction: time point x (t = 50 fluorescence) / time point 0 (t = 50 fluorescence) * 100% = % TCO intact. Peptide **8** was insoluble in these reactions and gave therefore no fluorescent intensity above background signal. Peptide **9** and **12** were both stable in serum up to 4 h and in complete medium gave ±25% response after 26 hours.

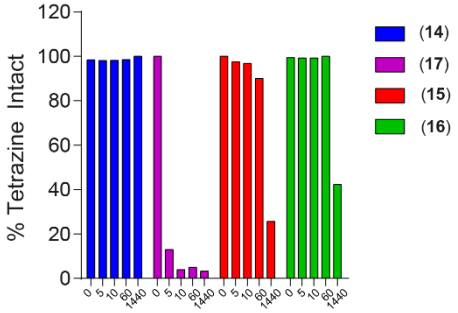

Figure S2 Tetrazine stability in serum. Stability of tetrazines were determined by incubation in Fetal Calf Serum (FCS) at room temperature, after which the characteristic absorption of tetrazines at 515 nm was quantified. At indicated times the absorption was measured and the tetrazine stability was determined with the following formula: time point x (absorption) / time point 0 (absorption) * 100% = % tetrazine intact. Tetrazine **17** is very unstable in serum while tetrazine **14** is very stable. After 24 hours 25% of **15** and 40% of **16** were still intact.

4.5 Experimental procedures

General methods: The synthesis of TCO carbonate **2** and bifunctional CCO/TCO carbonates **3** and **4** are described in Chapter 3 and 2, respectively. Dextran-modified tetrazine **21** was provided by Tagworks Pharmaceuticals.[30] Bodipy-tetrazine (**22**) was purchased from lumiprobe.com. Commercially available reagents and solvents were used as received. Moisture and oxygen sensitive reactions were performed under N_2 atmosphere (balloon). DCM, toluene, THF, dioxane and Et_2O were stored over (flame-dried) 4 Å molecular sieves (8-12 mesh). DIPEA and Et_3N were stored over KOH pellets. TLC analysis was performed using aluminum sheets, pre-coated with silica gel (Merck, TLC Silica gel 60 F_{254}). Compounds were visualized by UV absorption (λ = 254 nm), by spraying with either a solution of $KMnO_4$ (20 g/L) and K_2CO_3 (10 g/L) in H_2O, a solution of $(NH_4)_6Mo_7O_{24} \cdot 4H_2O$ (25 g/L) and $(NH_4)_4Ce(SO_4)_4 \cdot 2H_2O$ (10 g/L) in 10% H_2SO_4, 20% H_2SO_4 in EtOH, or phosphomolybdic acid in EtOH (150 g/L), where appropriate, followed by charring at ca. 150°C. Column chromatography was performed on Screening Devices b.v. Silica Gel (particle size 40-63 µm, pore diameter 60 Å). ^1H, ^{13}C APT, ^1H COSY, and HSQC spectra were recorded with a Bruker AV-400 (400/100 MHz) or AV-500 (500/125 MHz) spectrometer. Chemical shifts are reported as δ values (ppm) and were referenced to tetramethylsilane (δ = 0.00 ppm) or the residual solvent peak as internal standard. *J* couplings are reported in Hz.

LC-MS analysis was performed on a Finnigan Surveyor HPLC system (detection at 200-600 nm) with an analytical C_{18} column (Gemini, 50 x 4.6 mm, 3 µm particle size, Phenomenex) coupled to a Finnigan LCQ Advantage MAX ion-trap mass spectrometer (ESI^+). This system will be denoted "Setup A". Alternatively, LC-MS analysis was performed on an Agilent 1260 Infinity HPLC system (detection at 214 and 254 nm) with an analytical C_{18} column (Gemini, 50 x 4.6 mm, 3 µm particle size, Phenomenex) coupled to an Agilent 6120 quadrupole mass spectrometer (ESI^+). This system will be denoted "Setup B". In rare cases, this system was used with an analytical C_4 column (Gemini, 50 x 4.6 mm, 3 µm particle size, Phenomenex). For both LC-MS systems, the applied buffers were H_2O, MeCN and either 100 mM NH_4OAc in H_2O (10 mM NH_4OAc end concentration) or 1.0% TFA in H_2O (0.1% TFA end concentration). Methods used are: 10% → 90% MeCN, 13.5 min (0→0.5 min: 10% MeCN; 0.5→8.5 min: gradient time; 8.5→10.5 min: 90% MeCN; 10.5→13.5 min: 90% → 10% MeCN); 10% → 50% MeCN, 13.5 min (0→0.5 min: 10% MeCN; 0.5→8.5 min: gradient time; 8.5→10.5 min: 90% MeCN; 10.5→13.5 min: 90% → 10% MeCN); 0% → 50% MeCN, 13.5 min (0→0.5 min: 0% MeCN; 0.5→8.5 min: gradient time; 8.5→10.5 min: 50% MeCN; 10.5→13.5 min: 50% → 0% MeCN). HPLC purification was performed on a Gilson HPLC system (detection at 214 nm) coupled to a semi-preparative C_{18} column (Gemini, 250 x 10 mm, 5 µm particle size, Phenomenex). The applied buffers were H_2O, MeCN and either 100 mM NH_4OAc in H_2O (10 mM NH_4OAc end concentration) or 1.0% TFA in H_2O (0.1% TFA end concentration). High resolution mass spectra were recorded by direct injection (2 µL of a 2 µM solution in H_2O/MeCN 1:1 and 0.1% formic acid) on a mass spectrometer (Thermo Finnigan LTQ Orbitrap) equipped with an electrospray ion source in positive mode (source voltage 3.5 kV, sheath gas flow 10, capillary temperature 250°C) with resolution R = 60,000 at m/z 400 (mass range m/z = 150-2,000) and dioctylphthalate (m/z = 391.28428) as a "lock mass". The high resolution mass spectrometer was calibrated prior to measurements with a calibration mixture (Thermo Finnigan).

Photoisomerization methods: General guidelines were followed as described by Royzen *et al*.[53] Photochemical isomerization was performed using a Southern New England Ultraviolet Company Rayonet reactor (model RPR-100) equipped with 16 bulbs (part number RPR-2537A, λ = 254 nm). Photolysis was performed in a 1500 mL quartz flask (Southern New England Ultraviolet Company; part number RQV-323). A HPLC pump (Jasco; model PU-2088 Plus) was used to circulate solvent through the photolysis apparatus at the indicated flow rate. An empty solid load cartridge with screw cap, frits, O-ring and end tips (40 g; SD.0000.040; iLOK™, Screening Devices b.v.) was manually loaded with the specified silica gel to function as the stationary phase.

Peptide Synthesis. Peptide sequences were synthesized using Fmoc Solid Support Chemistry. The C-terminal amino acid was supported using a Wang resin. Elongation of the peptide sequence was accomplished using an automated and repetitive cycle of: *i.* 20% piperidine in NMP (Fmoc deprotection); *ii.* NMP wash; *iii.* Fmoc-protected amino acid (4 equiv), HCTU (4 equiv), DIPEA (8 equiv), NMP; *iv.* NMP wash; *v.* Ac_2O, DIPEA, NMP (capping); *vi.* NMP wash; *vii.* DCM wash. After completing the sequence, the N-terminal amino acid was also deprotected using 20% piperidine in NMP. An analytical amount of crude product was cleaved from the solid support (95% TFA, 2.5% H_2O, 2.5% TIS, > 1.5 h) and precipitated in cold, anhydrous Et_2O (TFA/Et_2O ≈ 1:10 *v/v*, wash resin once with TFA). The Et_2O solution was centrifuged, Et_2O was decanted and the pellet was dissolved in DMSO/MeCN/H_2O/*t*-BuOH (3:1:1:1 *v/v*) for LC-MS analysis.

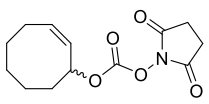

CCO carbonate 1: (Z)-Cyclooct-2-en-1-ol (Chapter 2 and 6; 276 mg, 2.19 mmol, 1.0 equiv) was placed under an argon atmosphere before dissolving in anhydrous MeCN (10 mL). N,N'-disuccinimidyl carbonate (672 mg, 2.62 mmol, 1.2 equiv) and DIPEA (0.46 ml, 2.62 mmol, 1.2 equiv) were added and the reaction mixture was stirred overnight at room temperature. TLC analysis indicated that the reaction was not complete; additional N,N'-disuccinimidyl carbonate (112 mg, 0.44 mmol, 0.2 equiv) and DIPEA (76 µL, 0.44 mmol, 0.2 equiv) were added and the reaction mixture was stirred overnight at room temperature. The reaction mixture was concentrated *in vacuo* and the crude product was purified by silica gel chromatography (20% → 30% EtOAc in pentane). The HOSu carbonate **1** (365 mg, 1.37 mmol, 62%) was obtained as a crystalline solid: R_f = 0.2 (20% EtOAc in pentane); ^{1}H NMR (400 MHz, $CDCl_3$) δ 5.81 – 5.70 (m, 1H), 5.64 – 5.54 (m, 2H), 2.82 (s, 4H), 2.22 – 2.12 (m, 2H), 2.12 – 2.01 (m, 1H), 1.73 – 1.34 (m, 7H); ^{13}C NMR (101 MHz, $CDCl_3$) δ 168.9 (x2), 151.2, 131.3, 128.6, 81.0, 34.8, 28.8, 26.5, 25.8, 25.6 (x2), 23.2.

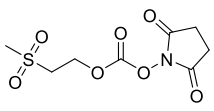

MSc-OSu (23): Synthesis was performed according to a modified procedure.[38] 2-(Methylsulfonyl)ethan-1-ol (2.03 g, 16.35 mmol, 1.0 equiv) was dissolved in anhydrous THF (40 mL) under N_2. The solution was cooled to 0°C (ice bath) before adding phosgene (20% *w/w* in toluene; 14 mL, 30.6 mmol, 1.9 equiv). After stirring for 30 min the reaction mixture was gradually warmed to room temperature and was stirred for an additional 4.5 h. The reaction mixture was concentrated *in vacuo* and the residual oil was cooled to -30°C under a N_2 atmosphere, resulting in crystallization of the acid chloride intermediate (2-(methylsulfonyl)ethyl carbonochloridate, **24**) which was used without further purification. N-

hydroxysuccinimide (1.88 g, 16.35 mmol, 1.0 equiv) was dissolved in anhydrous MeCN (16.35 mL) under a N_2 atmosphere. Et_3N (2.28 mL, 16.35 mmol, 1.0 equiv) was added and the solution was cooled to 0°C. A solution of the crude acid chloride (**24**) in MeCN (16 mL) was added dropwise to the reaction mixture. After 30 min, a precipitate ($Et_3N \cdot HCl$) was filtered off and the filtrate was concentrated *in vacuo*. A crystalline solid was precipitated from the crude product in warm isopropanol (~40°C). After filtration, the solid residue was recrystallized from MeCN to obtain MSc-OSu (**23**, 3.03 g, 11.44 mmol, 70%) as a white solid: ^{1}H NMR (400 MHz, CD_3CN) δ 4.68 (t, *J* = 5.5 Hz, 2H), 3.46 (t, *J* = 5.4 Hz, 2H), 2.94 (s, 3H), 2.75 (s, 4H); ^{13}C NMR (101 MHz, CD_3CN) δ 170.6 (x2), 152.1, 65.3, 53.5, 42.6, 26.2 (x2).

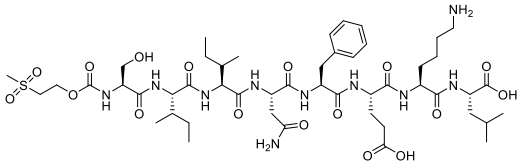

MSc-SIINFEKL (5): After SPPS, using 250 µmol Fmoc-Leu-Wang resin (1.0 equiv, based on theoretical resin loading), resin-bound SIINFEKL was washed with DCM (3 x 10 mL) and NMP (3 x 10 mL) before adding a solution of MSc-OSu (**23**, 331 mg, 1.25 mmol, 5.0 equiv) in NMP (6.0 mL). DIPEA (250 µL, 1 M in NMP, 1.0 equiv) was added and the resin suspension was shaken at room temperature for 3 h. The reaction mixture was drained and the resin-bound peptide was washed with NMP (3 x 10 mL) and DCM (3 x 10 mL). The crude product was cleaved from the solid support (95% TFA, 2.5% H_2O, 2.5% TIS, ~ 8 mL, > 1.5 h) and precipitated in cold, anhydrous Et_2O (TFA/Et_2O ≈ 1:10 *v/v*, wash resin once with TFA). The Et_2O suspension was centrifuged, Et_2O was decanted and an analytical amount of precipitated product was dissolved in DMSO/MeCN/H_2O/*t*-BuOH (3:1:1:1 *v/v*) for LC-MS analysis. The crude product was then purified with HPLC (30 → 45% MeCN in H_2O with 0.1% TFA) to obtain **5** (64.35 mg, 57.8 µmol, 23%) as a solid after lyophilization: LC-MS (setup B; linear gradient 10 → 90% MeCN, 0.1% TFA, 11 min): R_t (min): 4.74 (ESI-MS (m/z): 1113.6 ($M+H^+$)); HRMS: calculated for $C_{49}H_{81}N_{10}O_{17}S$ 1113.54964 $[M+H]^+$; found 1113.55101.

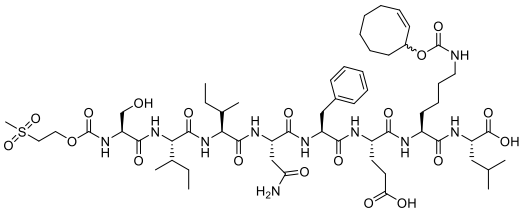

MSc-SIINFEK(CCO)L (25): MSc-SIINFEKL (**5**, 13.23 mg, 11.9 µmol, 1.0 equiv) and NHS-CCO (**1**, 4.13 mg, 15.5 µmol, 1.3 equiv) were combined in an Eppendorf tube (15 mL) and dissolved in anhydrous DMF (1.5 mL). Anhydrous DIPEA (8.30 µL, 48 µmol, 4 equiv) was added, the tube was briefly sonicated and flushed with N_2 before shaking the reaction mixture at room temperature. After 21 h, the reaction mixture was added to cold, anhydrous Et_2O (10 mL) to precipitate the product. The Et_2O suspension was centrifuged, Et_2O was decanted and the crude product **25** was dried over a stream of N_2 before using it in the next step without further purification: LC-MS (setup B; linear gradient 10 → 90% MeCN, 0.1% TFA, 11 min): R_t (min): 6.54 (ESI-MS (m/z): 1287.6 ($M+Na^+$), 1265.6 ($M+H^+$), 1113.6 (**5**$+H^+$)).

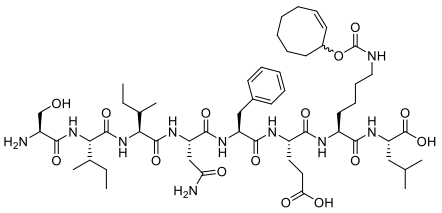

SIINFEK(CCO)L (6): The crude MSc-SIINFEK(CCO)L (**25**) previously described was dissolved in dioxane/MeOH/4 M NaOH (7.5:2.25:0.25 *v/v*, 12 mL). The reaction mixture was sonicated and occasionally shaken for 15 min. The reaction mixture was neutralized by adding acetic acid (68 µL, 1.2 mmol) before precipitating the product in cold, anhydrous Et_2O (~ 30 mL). The Et_2O suspension was centrifuged, Et_2O was decanted and the crude product **6** was dried over a stream of N_2. The crude product was then purified with HPLC (20 → 50% MeCN in H_2O with 10 mM NH_4OAc) to obtain **6** (2.15 mg, 1.93 µmol, 16% over two steps) as a solid after lyophilization: LC-MS (setup A; linear gradient 10 → 90% MeCN, 0.1% TFA, 12.5 min): R_t (min): 6.20 (ESI-MS (m/z): 1115.73 ($M+H^+$)). LC-MS (setup B; linear gradient 10 → 90% MeCN, 0.1% TFA, 11 min): R_t (min): 5.76 (diastereoisomer A, ESI-MS (m/z): 1115.6 ($M+H^+$), 963.5 (SIINFEKL+H^+)), 5.81 (diastereoisomer B, ESI-MS (m/z): 1115.6 ($M+H^+$), 963.5 (SIINFEKL+H^+)); HRMS: calculated for $C_{54}H_{87}N_{10}O_{15}$ 1115.63469 $[M+H]^+$; found 1115.63531.

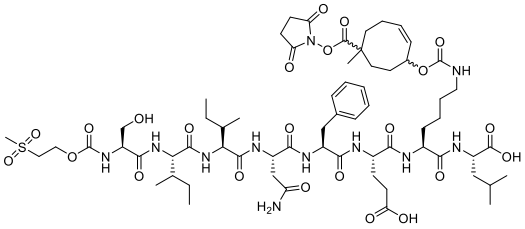

MSc-SIINFEK(NHS-bCCO)L (26): MSc-SIINFEKL (**5**, 40.4 mg, 36.3 µmol, 1.0 equiv) and NHS-bCCO (**3**, 21 mg, 50.0 µmol, 1.37 equiv) were combined in an Eppendorf tube (15 mL) and dissolved in anhydrous DMF (4.0 mL). Anhydrous DIPEA (25 µL, 145 µmol, 4.0 equiv) was added, the tube was briefly sonicated and flushed with N_2 before shaking the reaction mixture at room temperature. After 24 h, LC-MS indicated the desired product (**26**) to be the main reaction product. The reaction was continued without workup or purification: LC-MS (setup A; linear gradient 10 → 90% MeCN, 0.1% TFA, 12.5 min): R_t (min): 6.42 (ESI-MS (m/z): 1420.20 ($M+H^+$)).

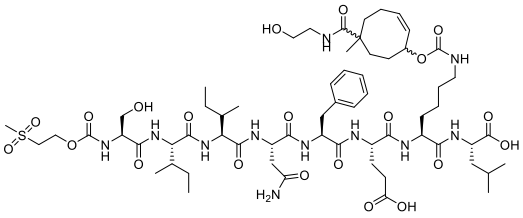

MSc-SIINFEK(mbCCO)L (27): Ethanolamine (8.78 µL, 145 µmol, 4.0 equiv) was added to the reaction mixture described for **26**. The reaction was shaken at room temperature. After 22 h, LC-MS indicated the desired product (**27**) to be the main reaction product. The reaction mixture was added to cold, anhydrous Et_2O (45 mL) to precipitate the product. The Et_2O suspension was centrifuged, Et_2O was decanted and the crude product **27** was dried over a stream of N_2 before using it in the next step without further purification: LC-MS (setup A; linear gradient 10 → 90% MeCN, 0.1% TFA, 12.5 min): R_t (min): 5.64 (ESI-MS (m/z): 1366.27 ($M+H^+$)).

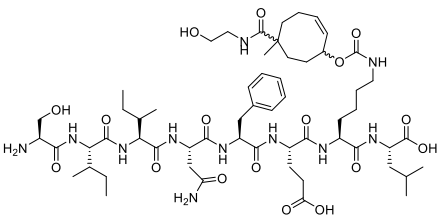

SIINFEK(mbCCO)L (7): The crude MSc-SIINFEK(mbCCO)L (**27**) previously described was dissolved in dioxane/MeOH/4 M NaOH (7.5:2.25:0.25 *v/v*, 35 mL). The reaction mixture was sonicated and occasionally shaken for 15 min. The reaction mixture was neutralized by adding acetic acid (206 µL, 3.6 mmol) before precipitating the product in cold, anhydrous Et_2O (~ 40 mL). The Et_2O suspension was centrifuged, Et_2O was decanted and the crude product **7** was dried over a stream of N_2. The crude product was then purified with HPLC (MeCN in H_2O with 10 mM NH_4OAc) to obtain **7** (8.3 mg, 6.82 µmol, 19% over three steps) as a solid after lyophilization: LC-MS (setup A; linear gradient 10 → 90% MeCN, 0.1% TFA, 12.5 min): R_t (min): 5.20 (ESI-MS (m/z): 1216.53 ($M+H^+$)); HRMS: calculated for $C_{58}H_{94}N_{11}O_{17}$ 1216.68237 $[M+H]^+$; found 1216.68220.

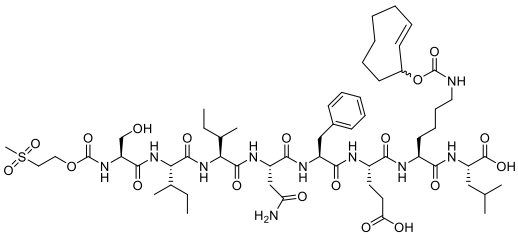

MSc-SIINFEK(TCO)L (28): MSc-SIINFEKL (**5**, 13.08 mg, 11.7 µmol, 1.0 equiv) and NHS-TCO (**2**, 4.24 mg, 15.9 µmol, 1.35 equiv) were combined in an Eppendorf tube (15 mL) and dissolved in anhydrous DMF (1.5 mL). Anhydrous DIPEA (8.21 µL, 47 µmol, 4 equiv) was added, the tube was briefly sonicated and flushed with N_2 before shaking the reaction mixture at room temperature. The Eppendorf tube was shielded with aluminum foil during the reaction. After 21 h, the reaction mixture was added to cold, anhydrous Et_2O (10 mL) to precipitate the product. The Et_2O suspension was centrifuged, Et_2O was decanted and the crude product **28** was dried over a stream of N_2 before using it in the next step without further purification: LC-MS (setup B; linear gradient 10 → 90% MeCN, 0.1% TFA, 11 min): R_t (min): 6.41 (ESI-MS (m/z): 1287.5 ($M+Na^+$), 1113.6 (**5**$+H^+$)).

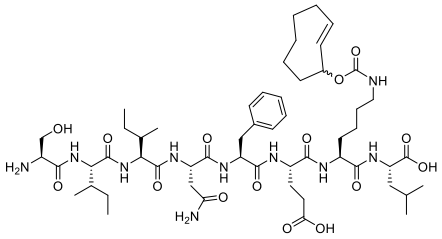

SIINFEK(TCO)L (8): The crude MSc-SIINFEK(TCO)L (**28**) previously described was dissolved in dioxane/MeOH/4 M NaOH (7.5:2.25:0.25 *v/v*, 12 mL). The reaction mixture was sonicated and occasionally shaken for 15 min. The reaction mixture was neutralized by adding acetic acid (67 µL, 1.2 mmol) before precipitating the product in cold, anhydrous Et_2O (~ 30 mL). The Et_2O suspension was centrifuged, Et_2O was decanted and the crude product **8** was dried over a stream of N_2. The crude product was then purified with HPLC (20 → 50% MeCN in H_2O with 10 mM NH4OAc) to obtain **8** (2.61 mg, 2.34 µmol, 20% over two steps) as a solid after lyophilization: LC-MS (setup A; linear gradient 10 → 90% MeCN, 0.1% TFA, 12.5 min): R_t (min): 6.06 (ESI-MS (m/z): 1115.80 ($M+H^+$), 1137.80 ($M+Na^+$)). LC-MS (setup B; linear gradient 10 → 90% MeCN, 0.1% TFA, 11 min): R_t (min): 5.66 (ESI-MS (m/z): 1115.6 ($M+H^+$), 963.6 (SIINFEKL$+H^+$)); HRMS: calculated for $C_{54}H_{87}N_{10}O_{15}$ 1115.63469 $[M+H]^+$; found 1115.63502.

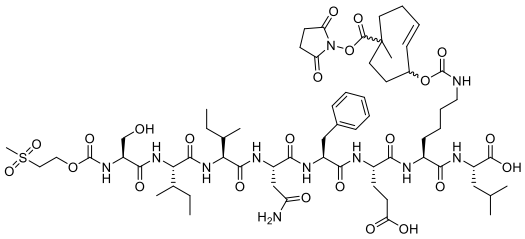

MSc-SIINFEK(NHS-bTCO)L (29): MSc-SIINFEKL (**5**, 12.15 mg, 10.91 µmol, 1.0 equiv) and NHS-bTCO (**4**, 5.53 mg, 13.09 µmol, 1.2 equiv) were combined in an Eppendorf tube (15 mL) and dissolved in anhydrous DMF (1.5 mL). Anhydrous DIPEA (7.62 µL, 43.64 µmol, 4.0 equiv) was added, the tube was briefly sonicated and flushed with N_2 before shaking the reaction mixture at room temperature. The Eppendorf tube was shielded with aluminum foil during the reaction. After 20 h, the reaction mixture was added to cold, anhydrous Et_2O (10 mL) to precipitate the product. The Et_2O suspension was centrifuged, Et_2O was decanted and the crude product **29** was dried over a stream of N_2 before using it in the next step without further purification: LC-MS (setup A; linear gradient 10 → 90% MeCN, 0.1% TFA, 12.5 min): R_t (min): 6.52 (ESI-MS (m/z): 1420.13 ($M+H^+$)).

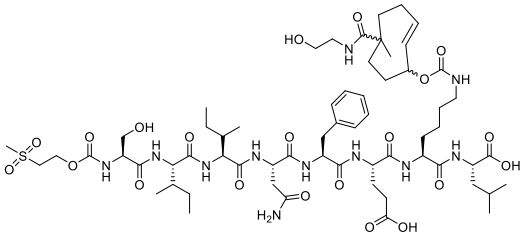

MSc-SIINFEK(mbTCO)L (30): The crude MSc-SIINFEK(NHS-bTCO)L (**29**) previously described was dissolved in anhydrous DMF (1.5 mL). Ethanolamine (2.63 µL, 43.71 µmol, 4.0 equiv) was added, the tube was briefly sonicated and flushed with N_2 before shaking the reaction mixture at room temperature. The Eppendorf tube was shielded with aluminum foil during the reaction. After 22 h, the reaction mixture was added to cold, anhydrous Et_2O (10 mL) to precipitate the product. The Et_2O suspension was centrifuged, Et_2O was decanted and the crude product **30** was dried over a stream of N_2 before using it in the next step without further purification: LC-MS (setup B with C_4 column; linear gradient 10 → 90% MeCN, 0.1% TFA, 11 min): R_t (min): 4.93 (ESI-MS (m/z): 1366.6 ($M+H^+$), 1113.5 (**5**$+H^+$).

Note: synthesis of **30 from **5** could also be performed without work-up after LC-MS analysis indicated the first step was complete.*

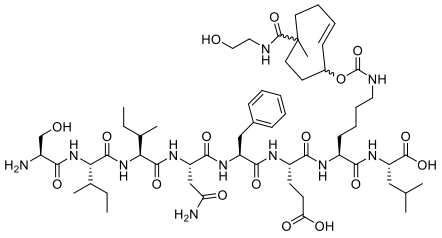

SIINFEK(mbTCO)L (9): The crude MSc-SIINFEK(mbTCO)L (**30**) previously described was dissolved in dioxane/MeOH/4 M NaOH (7.5:2.25:0.25 *v/v*, 10.9 mL). The reaction mixture was sonicated and occasionally shaken for 15 min. The reaction mixture was neutralized by adding acetic acid (62 µL, 1.09 mmol) before precipitating the product in cold, anhydrous Et_2O (~ 30 mL). The Et_2O suspension was centrifuged, Et_2O was decanted and the crude product **9** was dried over a stream of N_2. The crude product was then purified with HPLC (20 → 55% MeCN in H_2O with 10 mM NH_4OAc) to obtain **9** (1.81 mg, 1.49 µmol, 14% over three steps) as a solid after lyophilization: LC-MS (setup A; linear gradient 10 →

90% MeCN, 0.1% TFA, 12.5 min): R_t (min): 5.23 (ESI-MS (m/z): 1216.40 ($M+H^+$)); HRMS: calculated for $C_{58}H_{94}N_{11}O_{17}$ 1216.68237 $[M+H]^+$; found 1216.68391.

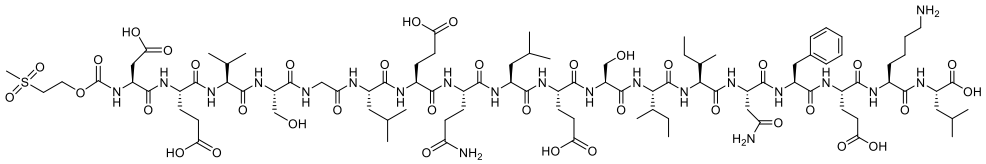

MSc- DEVSGLEQLESIINFEKL (10): After SPPS, using 250 µmol Fmoc-Leu-Wang resin (1.0 equiv, based on theoretical resin loading), resin bound DEVSGLEQLESIINFEKL was washed with DCM (3 x 10 mL) and NMP (3 x 10 mL) before adding a solution of MSc-OSu (**23**, 332 mg, 1.25 mmol, 5.0 equiv) in NMP (6 mL). DIPEA (250 µL, 1 M in NMP, 1.0 equiv) was added and the resin suspension was shaken at room temperature for 4 h. The reaction mixture was drained, MSc-OSu (**23**, 332 mg, 1.25 mmol, 5.0 equiv) in NMP (6 mL) and DIPEA (250 µL, 1 M in NMP, 1.0 equiv) were added and the resin suspension was shaken for an additional 2 h. The reaction mixture was drained and the resin-bound peptide was washed with NMP (3 x 10 ml) and DCM (3 x 10 ml). The crude product was cleaved from the solid support (95% TFA, 2.5% H_2O and 2.5% TIS, ~ 6 mL, > 1.5 h) and precipitated in cold, anhydrous Et_2O (TFA/Et_2O ≈ 1:10 *v/v*, wash resin once with TFA). The Et_2O suspension was centrifuged, Et_2O was decanted and an analytical amount of precipitated product was dissolved in DMSO/MeCN/H_2O/*t*-BuOH (3:1:1:1 *v/v*) for LC-MS analysis. The crude product was purified with HPLC (25 → 50% MeCN in H_2O with 0,1% TFA) to obtain **10** (80 mg, 36 µmol, 14%) as a solid after lyophilization: LC-MS (setup A; linear gradient 10 → 90% MeCN, 0.1% TFA, 11 min): R_t (min): 5.66 (ESI-MS (m/z): 1107.47 ($M+2H^+$)).

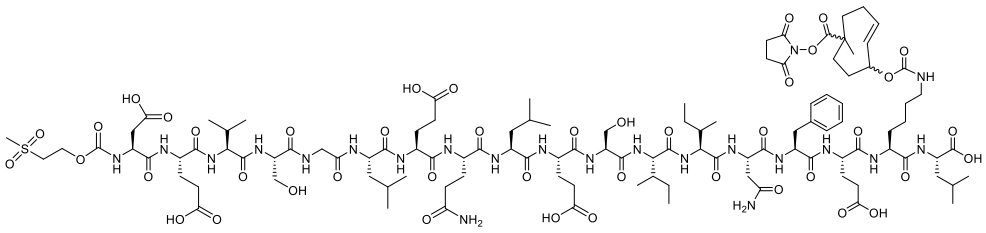

MSc-DEVSGLEQLESIINFEK(NHS-bTCO)L (31): MSc-DEVSGLEQLESIINFEKL (**10**, 20 mg, 9.04 µmol, 1.0 equiv) and NHS-bTCO(**4**, 8.7 mg, 21 µmol, 2.3 equiv) were combined in an Eppendorf tube (15 mL) and dissolved in DMSO (1.5 mL). Anhydrous DIPEA (15 µL, 86 µmol, 9.5 equiv) was added, the tube was briefly sonicated and flushed with N_2 before shaking the reaction mixture at room temperature. The Eppendorf tube was shielded with aluminum foil during the reaction. After 20 h, the reaction mixture was added to cold, anhydrous Et_2O (45 ml) to precipitate the product. The Et_2O suspension was briefly centrifuged, Et_2O was decanted and the crude product **31** was dried over a stream of N_2 before using it in the next step without further purification: LC-MS (setup A; linear gradient 10 → 90% MeCN, 0.1% TFA, 11 min): R_t (min): 6.56 (ESI-MS (m/z): 1260.67 ($M+2H^+$)).

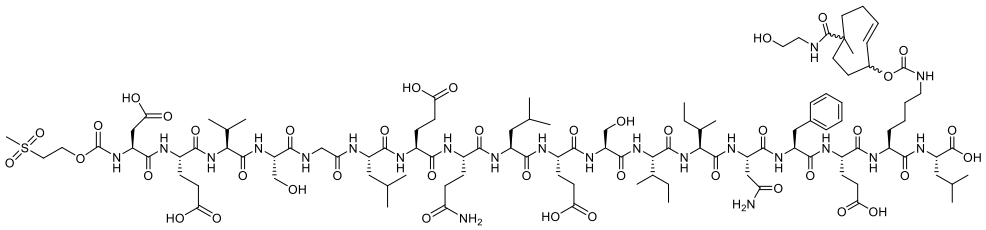

MSc-DEVSGLEQLESIINFEK(mbTCO)L (32): The crude MSc-DEVSGLEQLESIINFEK(NHS-bTCO)L (**31**) preciously described was dissolved in DMSO (1.5 mL). Ethanolamine (5.0 µL, 83 µmol, 9.2 equiv) was added, the tube was briefly sonicated and flushed with N_2 before shaking the reaction mixture at room temperature. The Eppendorf tube was shielded with aluminum foil during the reaction. After 20 h, the reaction mixture was added to cold, anhydrous Et_2O (45 ml) to precipitate the product. The Et_2O suspension was briefly centrifuged, Et_2O was decanted and the crude product **32** was dried over a stream of N_2 before using it in the next step without further purification: LC-MS (setup A; linear gradient 10 → 90% MeCN, 0.1% TFA, 11 min): R_t (min): 6.07 (ESI-MS (m/z): 1233.87 ($M+2H^+$)).

Note: synthesis of **32 from **10** could also be performed without work-up after LC-MS analysis indicated the first step was complete.*

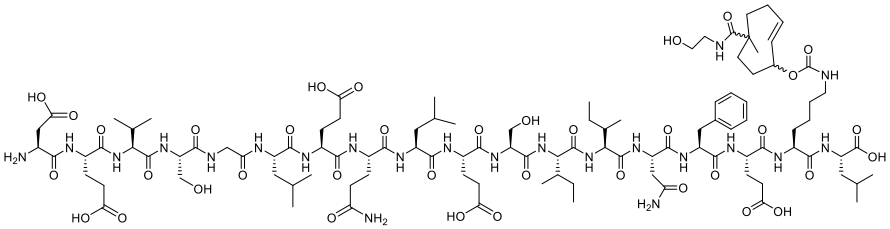

DEVSGLEQLESIINFEK(mbTCO)L (11): The crude MSc-DEVSGLEQLESIINFEK(mbTCO)L (**32**) preciously described was dissolved in dioxane/MeOH/4 M NaOH (7.5:2.25:0.25 *v/v*, 10 mL). The reaction mixture was sonicated and occasionally shaken for 15 min. The reaction mixture was neutralized by adding acetic acid (54 µL, 0.94 mmol) before precipitating the product in cold, anhydrous Et_2O (~ 40 mL). The Et_2O suspension was centrifuged, Et_2O was decanted and the crude product **11** was dried over a stream of N_2. The crude product was then purified with HPLC (25 → 50% MeCN in H_2O with 10 mM NH_4OAc) to obtain **11** (8.6 mg, 3.71 µmol, 41% over three steps) as a solid after lyophilization: LC-MS (setup A; linear gradient 10 → 90% MeCN, 0.1% TFA, 11 min): R_t (min): 5.53 (ESI-MS (m/z): 1158.73 ($M+2H^+$)); HRMS: calculated for $C_{104}H_{168}N_{22}O_{37}$ 1158.59649 $[M+2H]^{2+}$; found 1158.59632.

Note: during HPLC purification of **11, addition of NH_4OAc can increase the quantities of crude product injected per run.*

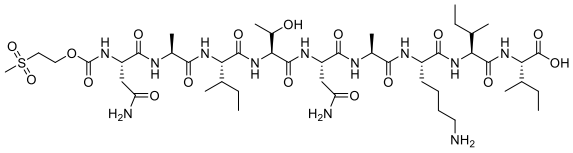

MSc-NAITNAKII (13): After SPPS, using 250 µmol Fmoc-Ile-Wang resin (1.0 equiv, based on theoretical resin loading), resin-bound NAITNAKII was washed with DCM (3 x 10 mL) and NMP (3 x 10 mL) before adding a solution of MSc-OSu (**23**, 331 mg, 1.25 mmol, 5.0 equiv) in NMP (6.0 mL). DIPEA (250 µL, 1 M in NMP, 1.0 equiv) was added and the reaction mixture was stirred at room temperature for 3 h. The reaction mixture was drained and the resin-bound peptide was washed with NMP (3 x 10 mL) and DCM (3 x 10 mL). The crude product was cleaved from the solid support (95% TFA, 2.5% H_2O, 2.5% TIS, ~ 8 mL, > 1.5 h) and precipitated in cold, anhydrous Et_2O (TFA/Et_2O ≈ 1:10 *v/v*, wash resin once with TFA). The Et_2O suspension was centrifuged, Et_2O was decanted and an analytical amount of precipitated product was dissolved in DMSO/MeCN/H_2O/*t*-BuOH (3:1:1:1 *v/v*) for LC-MS analysis. The crude product was then purified with HPLC (30 → 45% MeCN in H_2O with 0.1% TFA) to obtain **13** (43.5 mg, 39.3 µmol, 16%) as a solid after lyophilisation. The purified product still contained a capped byproduct of the SPPS. LC-MS (setup B; linear gradient 10 → 90% MeCN, 0.1% TFA, 11 min): R_t (min): 3.91 (ESI-MS (m/z): 885.5 (Acetyl-AITNAKII+H^+)), 4.05 (ESI-MS (m/z): 1107.5 (M+H^+)); HRMS: calculated for $C_{46}H_{83}N_{12}O_{17}S$ 1107.57144 $[M+H]^+$; found 1107.57213.

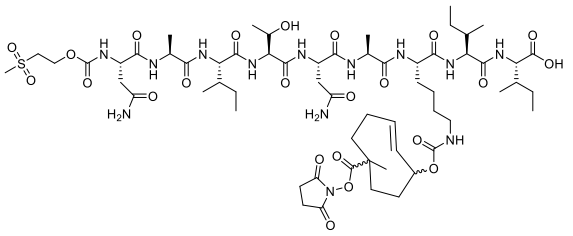

MSc-NAITNAK(NHS-bTCO)II (33): MSc-NAITNAKII (**13**, 11.15 mg, 10.07 µmol, 1.0 equiv) and NHS-bTCO (**4**, 5.57 mg, 13.19 µmol, 1.3 equiv) were combined in an Eppendorf tube (15 mL) and dissolved in anhydrous DMF (1.5 mL). Anhydrous DIPEA (7.03 µL, 40.31 µmol, 4 equiv) was added, the tube was briefly sonicated and flushed with N_2 before shaking the reaction mixture at room temperature. The Eppendorf tube was shielded with aluminum foil during the reaction. After 23 h, the reaction mixture was added to cold, anhydrous Et_2O (12 mL) to precipitate the product. The Et_2O suspension was centrifuged, Et_2O was decanted and the crude product **33** was dried over a stream of N_2 before using it in the next step without further purification: LC-MS (setup A; linear gradient 10 → 90% MeCN, 0.1% TFA, 12.5 min): R_t (min): 6.01 (ESI-MS (m/z): 1414.60 (M+H^+)).

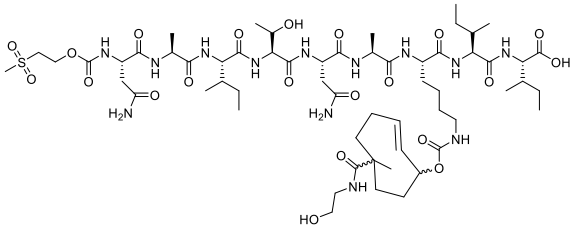

MSc-NAITNAK(mbTCO)II (34): The crude MSc-NAITNAK(NHS-bTCO)II (**33**) previously described was dissolved in anhydrous DMF (1.4 mL). Ethanolamine (2.44 µL, 40.27 µmol, 4 equiv) was added, the tube was briefly sonicated and flushed with N_2 before shaking the reaction mixture at room temperature. The Eppendorf tube was shielded with aluminum foil during the reaction. After 24 h, the reaction mixture was added to cold, anhydrous

Et_2O (12 mL) to precipitate the product. The Et_2O suspension was centrifuged, Et_2O was decanted and the crude product **34** was dried over a stream of N_2 before using it in the next step without further purification: LC-MS (Setup A; linear gradient 10 → 90% MeCN, 0.1% TFA, 11 min): R_t (min): 5.23 (ESI-MS (m/z): 1360.67 ($M+H^+$)).

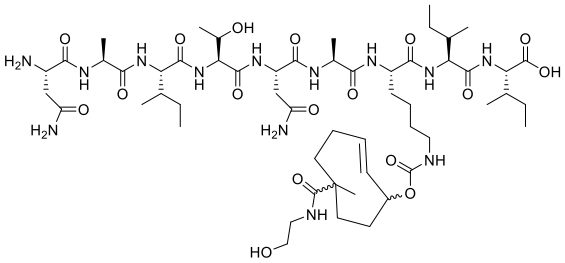

NAITNAK(mbTCO)II (12): The crude MSc-NAITNAK(mbTCO)II (**34**) previously described was dissolved in dioxane/MeOH/4 M NaOH (7.5:2.25:0.25 *v/v*, 10 mL). The reaction mixture was sonicated and occasionally shaken for 15 min. The reaction mixture was neutralized by adding acetic acid (58 µL, 1.01 mmol) before precipitating the product in cold, anhydrous Et_2O (~ 30 mL). The Et_2O suspension was centrifuged, Et_2O was decanted and the crude product **12** was dried over a stream of N_2. The crude product was then purified with HPLC (10 → 30% MeCN in H_2O with 10 mM NH_4OAc) to obtain **12** (1.56 mg, 1.29 µmol, 13% over three steps) as a solid after lyophilization: LC-MS (setup A; linear gradient 10 → 50% MeCN, 0.1% TFA, 12.5 min): R_t (min): 6.15 (diastereoisomer A, ESI-MS (m/z): 1210.80 ($M+H^+$), 6.60 (diastereoisomer B, ESI-MS (m/z): 1210.80 ($M+H^+$)); HRMS: calculated for $C_{55}H_{96}N_{13}O_{17}$ 1210.70416 $[M+H]^+$; found 1210.70437.

General procedure for oxidizing dihydrotetrazines with NO_2 gas: A solution of HNO_3 (70% *w/w*) in H_2O (1:1 *v/v*, 20 mL) was added dropwise to a copper coin (3.65 g, 57.4 mmol) in H_2O (5 mL). The NO_2 gas formed was led through a cannula into the tetrazine reaction mixture. After the formation of NO_2 was visible, the reaction mixture was cooled to 0°C (for tetrazine **14**, this also serves to reduce evaporation of product from the reaction mixture) and the flow of NO_2 was stimulated with an argon/N_2 balloon. The process was continued until the copper was completely dissolved and all nitrous gasses were led through the reaction mixture. In case the copper oxidation does not go to completion, additional HNO_3 (70% *w/w*) can be added dropwise to the flask containing the copper.

General procedure for HRMS analysis of tetrazines: A solution of tetrazine (10 µL, **14**, **15**, **16** or **17**, 10 mM in DMSO) was added to a solution of axial 4-TCO-OH[53,54] (1 µL, 100 mM in DMSO). The reaction mixture was diluted with MeCN/H_2O/*t*-BuOH (1:1:1 *v/v*; 90 µL) and subjected to HRMS analysis of the corresponding IEDDA adduct.

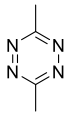

3,6-dimethyl-1,2,4,5-tetrazine (14): Acetamidine hydrochloride (**18**, 3.97 g, 42 mmol, 1.0 equiv) was dissolved in H_2O (20 mL). Hydrazine hydrate (4.12 mL, 84 mmol, 2.0 equiv) was added and the solution was stirred at room temperature. After stirring for 3.5 h, the reaction mixture was oxidized with NO_2 gas. When the formation of NO_2 gas stopped, the deep-red reaction mixture (pH ~ 10) was acidified with HCl (1 M, 100 mL) and extracted with DCM (3 x 75 mL). The combined organic layers were washed with HCl (1 M, 100 mL), dried over $MgSO_4$, filtered and concentrated *in vacuo* to yield 3,6-dimethyl-1,2,4,5-tetrazine (**14**, 425 mg, 3.86 mmol, 18%) as deep-purple crystals: ^1H NMR (400 MHz, $CDCl_3$) δ 3.04 (s, 6H);

^{13}C NMR (101 MHz, $CDCl_3$) δ 167.3 (x2), 21.1 (x2); HRMS (IEDDA adduct with axial 4-TCO-OH): calculated for $C_{12}H_{21}N_2O$ 209.16484 $[M+H]^+$; found 209.16469. A trace of the intermediate product, 3,6-dimethyl-1,4-dihydro-1,2,4,5-tetrazine, was visible on ^{1}H and ^{13}C NMR. Spectroscopic data was in agreement with literature.[26]

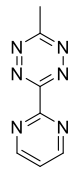

3-methyl-6-(pyrimidin-2-yl)-1,2,4,5-tetrazine (15): Synthesis was performed according to a modified procedure.[27] Pyrimidine-2-carbonitrile (**19**, 2.10 g, 20 mmol, 1.0 equiv) and zinc trifluoromethanesulfonate (1.82 g, 5.0 mmol, 0.25 equiv) were combined in a point-bottom flask before adding MeCN (5.22 mL, 100 mmol, 5.0 equiv) and hydrazine monohydrate (4.85 mL, 100 mmol, 5.0 equiv). The reaction mixture was stirred at 60°C (oil bath) under a positive N_2 gas stream. After 7 h, additional MeCN (2.5 mL, 47.9 mmol, 2.4 equiv) was added. After 24 h, the crude reaction mixture was dissolved in HCl (0.5 M, 40 mL) before oxidation with NO_2 gas. When the formation of NO_2 gas stopped, HCl (1 M, 100 mL) was added and the reaction mixture was extracted with DCM (3 x 75 mL). The combined organic layers were washed with HCl (1 M, 150 mL), dried over $MgSO_4$, filtered and concentrated *in vacuo*. The crude product was purified by silica gel chromatography (0% → 2% → 3% MeOH in DCM) to obtain 3-methyl-6-(pyrimidin-2-yl)-1,2,4,5-tetrazine (**15**, 1.09 g, 6.26 mmol, 31%) as deep-purple crystals: R_f = 0.2 (2% MeOH in DCM); ^{1}H NMR (400 MHz, $CDCl_3$) δ 9.14 (d, *J* = 4.9 Hz, 2H), 7.62 (t, *J* = 4.9 Hz, 1H), 3.24 (s, 3H); ^{13}C NMR (101 MHz, $CDCl_3$) δ 168.8, 163.3, 159.5, 158.5, 122.6, 21.6; HRMS (IEDDA adduct with axial 4-TCO-OH): calculated for $C_{15}H_{21}N_4O$ 273.17099 $[M+H]^+$; found 273.17078. Spectroscopic data was in agreement with literature.[27]

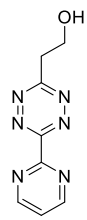

2-(6-(pyrimidin-2-yl)-1,2,4,5-tetrazin-3-yl)ethan-1-ol (16): Synthesis was performed according to literature reference.[27] Pyrimidine-2-carbonitrile (**19**, 2.10 g, 20 mmol, 1.0 equiv) and zinc trifluoromethanesulfonate (1.82 g, 5.0 mmol, 0.25 equiv) were combined in a point-bottom flask before adding 3-hydroxypropanenitrile (6.84 mL, 100 mmol, 5.0 equiv) and hydrazine monohydrate (4.85 mL, 100 mmol, 5.0 equiv). The reaction mixture was stirred at 60°C (oil bath) under a positive N_2 gas stream. After 24 h, the reaction mixture was dissolved into a solution of sodium nitrite (1 M, 200 mL). The resulting mixture was acidified to pH ~ 3 by slowly adding HCl (1 M). The mixture was extracted with DCM (3 x 150 mL) and the combined organic layers were washed with brine (~ 250 mL), dried over $MgSO_4$, filtered and concentrated *in vacuo*. The crude product was purified by silica gel chromatography (0% → 3% MeOH in DCM) and subsequent crystallization from EtOAc to obtain 2-(6-(pyrimidin-2-yl)-1,2,4,5-tetrazin-3-yl)ethan-1-ol (**16**, 142 mg, 0.70 mmol, 3%) as pink crystals: R_f = 0.2 (3% MeOH in DCM); ^{1}H NMR (400 MHz, $CDCl_3$) δ 9.13 (d, *J* = 4.8 Hz, 2H), 7.61 (t, *J* = 4.8 Hz, 1H), 4.37 (t, *J* = 5.8 Hz, 2H), 3.76 (t, *J* = 5.8 Hz, 2H), 2.80 (s, 1H); ^{13}C NMR (101 MHz, $CDCl_3$) δ 169.9, 163.6, 159.4, 158.6 (x2), 122.8, 60.1, 38.0; HRMS (IEDDA adduct with axial 4-TCO-OH): calculated for $C_{16}H_{23}N_4O_2$ 303.18155 $[M+H]^+$; found 303.18141. Spectroscopic data was in agreement with literature.[27]

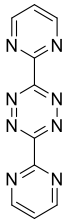

3,6-di(pyrimidin-2-yl)-1,2,4,5-tetrazine (17): Synthesis was performed according to literature reference.[43] Pyrimidine-2-carbonitrile (**19**, 3.00 g, 28.5 mmol, 1.0 equiv) and HCl (37% *w/w*, 4.5 mL, 56.3 mmol, 2.0 equiv) were dissolved in THF (40 mL). Hydrazine hydrate (8.0 mL, 165 mmol, 5.8 equiv) was added dropwise and the resulting mixture was stirred under reflux overnight. Conversion of **19** into the dihydrotetrazine intermediate (3,6-di(pyrimidin-2-yl)-1,4-dihydro-1,2,4,5-tetrazine, **20**, R_f = 0.5 (5% MeOH in DCM)) was shown using TLC. H_2O (40 mL) was added and THF was evaporated *in vacuo* (up to ~ 150 mbar, 40°C) before extracting the reaction mixture with DCM (~ 2 – 3 L total). The combined organic layers were concentrated *in vacuo* to yield the orange dihydrotetrazine intermediate (**20**) as an orange solid. The intermediate product was dissolved in DMF (100 mL) before oxidation with NO_2 gas. During oxidation, a purple precipitate was formed which was filtrated after ~ 45 min and washed twice with ice cold H_2O. The purple precipitate (2.38 g) was recrystallized from $CHCl_3$ to obtain 3,6-di(pyrimidin-2-yl)-1,2,4,5-tetrazine (**17**, 0.95 g, 3.99 mmol, 14%) as a purple solid: ^{1}H NMR (400 MHz, $CDCl_3$) δ 9.19 (d, *J* = 4.9 Hz, 4H), 7.64 (t, *J* = 4.9 Hz, 2H); ^{13}C NMR (126 MHz, $CDCl_3$) δ 163.9 (x2), 159.5 (x2), 158.7 (x4), 122.9 (x2); HRMS (IEDDA adduct with axial 4-TCO-OH): calculated for $C_{18}H_{21}N_6O$ 337.17714 $[M+H]^+$; found 337.17707. Spectroscopic data was in agreement with literature.[43]

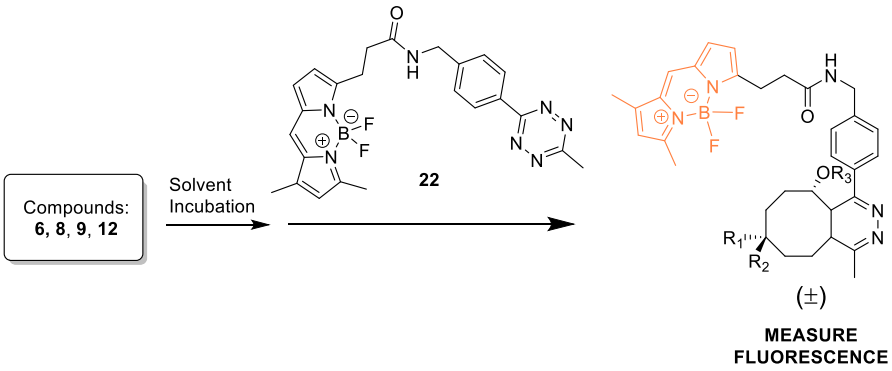

Stability of TCO constructs (Figure S1): Stability of TCO constructs were determined by incubation in the desired solvent (Full Medium or Fetal Calf Serum) at 37°C over a time period of 24 h. 30 µl of a 200 µM solution of TCO-construct (**6**, **8**, **9**, **12**) in DMSO was dissolved in 2970 µl solvent. The resulting 2 µM solution was incubated at 37°C. At time points 0, 1, 2, 3, 4 and 24 h three times 100 µl was transferred to separate wells in a Greiner flat black 96 well plate and each was diluted with 100 µl of a freshly prepared solution of Bodipy-Tz **22** (10 µM), resulting in three 200 µl solutions (1 µM TCO-construct, 5 µM Bodipy-Tz **22**). Solution fluorescence was measured using a Tecan Infinite M1000 Pro (λ_{ex} = 491 nm, λ_{em} = 525 nm) for 60 minutes at 1 min intervals and TCO stability was determined as a relative percentage to time point 0 (for each compound individually). Control samples containing 100 µl solvent (1% DMSO) were diluted with 100 µl Bodipy-Tz (**22**, 10 µM) and measured at all time points to establish a baseline. Formula after baseline correction:

Time point x (t = 50 fluorescence) / time point 0 (t = 50 fluorescence) * 100% = % TCO intact.

Stability of tetrazines (Figure S2): Stability of tetrazines were determined by incubation in Fetal Calf Serum (FCS) at room temperature. 10 µl of a 100 mM solution of tetrazine (**14** – **17**) in DMSO was dissolved in 990 µl FCS. Intact tetrazine present in the resulting 1 mM solution was quantified by the intensity of its characteristic absorption at 515 nm. After initial mixing of the sample, 500 µl was measured at time points 0, 1, 5, 10 and 60 min, and the remaining 500 µl was measured after 24 h. A control solvent sample (1% DMSO) was measured initially at 0 min and 24 h to establish a 0% value. Formula after 0% correction:

Time point x (absorption) / time point 0 (absorption) * 100% = % tetrazine intact.

4.6 References

[1] A. Lanzavecchia, *Nature* **1998**, *393*, 413–414.

[2] S. D. Rosen, *Annu. Rev. Immunol.* **2004**, *22*, 129–156.

[3] J. W. Yewdell, E. Reits, J. Neefjes, *Nat. Rev. Immunol.* **2003**, *3*, 952–961.

[4] T. N. Schumacher, R. D. Schreiber, *Science* **2015**, *348*, 69–74.

[5] J. Neefjes, M. L. Jongsma, P. Paul, O. Bakke, *Nat Rev Immunol* **2011**, *11*, 823–36.

[6] O. P. Joffre, E. Segura, A. Savina, S. Amigorena, *Nat. Rev. Immunol.* **2012**, *12*, 557–569.

[7] D. J. Irvine, M. A. Purbhoo, M. Krogsgaard, M. M. Davis, *Nature* **2002**, *419*, 845–849.

[8] R. N. Germain, *FEBS Lett.* **2010**, *584*, 4814–4822.

[9] J. Huang, M. Brameshuber, X. Zeng, J. Xie, Q. Li, Y. Chien, S. Valitutti, M. M. Davis, *Immunity* **2013**, *39*, 846–857.

[10] G. Altan-Bonnet, R. N. Germain, *PLoS Biol.* **2005**, *3*, e356.

[11] D. Zehn, S. Y. Lee, M. J. Bevan, *Nature* **2009**, *458*, 211–214.

[12] R. H. Schwartz, *Annu. Rev. Immunol.* **1985**, *3*, 237–261.

[13] J. B. Pawlak, B. J. Hos, M. J. van de Graaff, O. A. Megantari, N. Meeuwenoord, H. S. Overkleeft, D. V. Filippov, F. Ossendorp, S. I. van Kasteren, *ACS Chem. Biol.* **2016**, *11*, 3172–3178.

[14] J. B. Pawlak, G. P. P. Gential, T. J. Ruckwardt, J. S. Bremmers, N. J. Meeuwenoord, F. A. Ossendorp, H. S. Overkleeft, D. V. Filippov, S. I. van Kasteren, *Angew. Chem. Int. Ed.* **2015**, *54*, 5628–5631.

[15] J. D. Stone, A. S. Chervin, D. M. Kranz, *Immunology* **2009**, *126*, 165–176.

[16] D. Lodygin, A. Flügel, *Cell Calcium* **2017**, *64*, 118–129.

[17] K. A. Markey, K. H. Gartlan, R. D. Kuns, K. P. A. MacDonald, G. R. Hill, *J. Immunol. Methods* **2015**, *423*, 40–44.

[18] G. A. Azar, F. Lemaître, E. A. Robey, P. Bousso, *Proc. Natl. Acad. Sci.* **2010**, *107*, 3675–3680.

[19] T. R. Mempel, S. E. Henrickson, U. H. von Andrian, *Nature* **2004**, *427*, 154–159.

[20] S. Halle, K. A. Keyser, F. R. Stahl, A. Busche, A. Marquardt, X. Zheng, M. Galla, V. Heissmeyer, K. Heller, J. Boelter, K. Wagner, Y. Bischoff, R. Martens, A. Braun, K. Werth, A. Uvarovskii, H. Kempf, M. Meyer-Hermann, R. Arens, M. Kremer, G. Sutter, M. Messerle, R.

Förster, *Immunity* **2016**, *44*, 233–245.

[21] A. L. DeMond, T. Starr, M. L. Dustin, J. T. Groves, *J. Am. Chem. Soc.* **2006**, *128*, 15354–15355.

[22] M. Huse, L. O. Klein, A. T. Girvin, J. M. Faraj, Q.-J. Li, M. S. Kuhns, M. M. Davis, *Immunity* **2007**, *27*, 76–88.

[23] J. Luo, Q. Liu, K. Morihiro, A. Deiters, *Nat. Chem.* **2016**, *8*, 1027–1034.

[24] J. Sauer, H. Wiest, *Angew. Chem.* **1962**, *74*, 353–353.

[25] M. L. Blackman, M. Royzen, J. M. Fox, *J. Am. Chem. Soc.* **2008**, *130*, 13518–13519.

[26] R. M. Versteegen, R. Rossin, W. ten Hoeve, H. M. Janssen, M. S. Robillard, *Angew. Chem. Int. Ed.* **2013**, *52*, 14112–14116.

[27] X. Fan, Y. Ge, F. Lin, Y. Yang, G. Zhang, W. S. C. Ngai, Z. Lin, S. Zheng, J. Wang, J. Zhao, J. Li, P. R. Chen, *Angew. Chem. Int. Ed.* **2016**, *55*, 14046–14050.

[28] J. C. T. Carlson, H. Mikula, R. Weissleder, *J. Am. Chem. Soc.* **2018**, *140*, 3603–3612.

[29] R. M. Versteegen, W. ten Hoeve, R. Rossin, M. A. R. de Geus, H. M. Janssen, M. S. Robillard, *Angew. Chem. Int. Ed.* **2018**, *57*, 10494–10499.

[30] R. Rossin, S. M. J. van Duijnhoven, W. ten Hoeve, H. M. Janssen, F. J. M. Hoeben, R. M. Versteegen, M. S. Robillard, *Bioconjug. Chem.* **2016**, *27*, 1697–1706.

[31] R. Rossin, R. M. Versteegen, J. Wu, A. Khasanov, H. J. Wessels, E. J. Steenbergen, W. ten Hoeve, H. M. Janssen, A. H. A. M. van Onzen, P. J. Hudson, M. S. Robillard, *Nat. Commun.* **2018**, *9*, 1484.

[32] G. Zhang, J. Li, R. Xie, X. Fan, Y. Liu, S. Zheng, Y. Ge, P. R. Chen, *ACS Cent. Sci.* **2016**, *2*, 325–331.

[33] J. M. Mejia Oneto, I. Khan, L. Seebald, M. Royzen, *ACS Cent. Sci.* **2016**, *2*, 476–482.

[34] M. Czuban, S. Srinivasan, N. A. Yee, E. Agustin, A. Koliszak, E. Miller, I. Khan, I. Quinones, H. Noory, C. Motola, R. Volkmer, M. Di Luca, A. Trampuz, M. Royzen, J. M. Mejia Oneto, *ACS Cent. Sci.* **2018**, *4*, 1624–1632.

[35] Q. Yao, F. Lin, X. Fan, Y. Wang, Y. Liu, Z. Liu, X. Jiang, P. R. Chen, Y. Gao, *Nat. Commun.* **2018**, *9*, 5032.

[36] J. Zhao, Y. Liu, F. Lin, W. Wang, S. Yang, Y. Ge, P. R. Chen, *ACS Cent. Sci.* **2019**, *5*, 145–152.

[37] D. H. Fremont, E. A. Stura, M. Matsumura, P. A. Peterson, I. A. Wilson, *Proc. Natl. Acad. Sci.* **1995**, *92*, 2479–2483.

[38] G. I. Tesser, I. C. Balvert-Geers, *Int. J. Pept. Protein Res.* **1975**, *7*, 295–305.

[39] J. A. Rutigliano, M. T. Rock, A. K. Johnson, J. E. Crowe, B. S. Graham, *Virology* **2005**, *337*, 335–343.

[40] R. Lozano, M. Naghavi, K. Foreman, S. Lim, K. Shibuya, V. Aboyans, J. Abraham, T. Adair, R. Aggarwal, S. Y. Ahn, M. A. AlMazroa, M. Alvarado, H. R. Anderson, L. M. Anderson, K. G. Andrews, C. Atkinson, L. M. Baddour, S. Barker-Collo, D. H. Bartels, M. L. Bell, E. J. Benjamin, D. Bennett, K. Bhalla, B. Bikbov, A. Bin Abdulhak, G. Birbeck, F. Blyth, I. Bolliger, S. Boufous, C. Bucello, M. Burch, P. Burney, J. Carapetis, H. Chen, D. Chou, S. S. Chugh, L. E. Coffeng, S. D. Colan, S. Colquhoun, K. E. Colson, J. Condon, M. D. Connor, L. T. Cooper, M. Corriere, M. Cortinovis, K. C. de Vaccaro, W. Couser, B. C. Cowie, M. H. Criqui, M. Cross, K. C. Dabhadkar, N. Dahodwala, D. De Leo, L. Degenhardt, A. Delossantos, J. Denenberg, D. C. Des Jarlais, S. D. Dharmaratne, E. R. Dorsey, T. Driscoll, H. Duber, B. Ebel, P. J. Erwin, P. Espindola, M. Ezzati, V. Feigin, A. D. Flaxman, M. H. Forouzanfar, F. G. R. Fowkes, R. Franklin, M. Fransen, M. K. Freeman, S. E. Gabriel, E. Gakidou, F. Gaspari, R. F. Gillum, D. Gonzalez-Medina, Y. A. Halasa, D. Haring, J. E. Harrison, R. Havmoeller, R. J. Hay, B. Hoen, P. J. Hotez, D. Hoy, K. H. Jacobsen, S. L. James, R. Jasrasaria, S. Jayaraman, N. Johns, G. Karthikeyan, N. Kassebaum, A. Keren, J.-P. Khoo, L. M. Knowlton, O. Kobusingye, A. Koranteng, R. Krishnamurthi, M. Lipnick, S. E. Lipshultz, S. L. Ohno, J. Mabweijano, M. F. MacIntyre, L. Mallinger, L. March, G. B. Marks, R. Marks, A. Matsumori, R. Matzopoulos, B. M. Mayosi, J. H. McAnulty, M. M. McDermott, J. McGrath, Z. A. Memish, G. A. Mensah, T. R. Merriman, C. Michaud, M. Miller, T. R. Miller, C. Mock, A. O. Mocumbi, A. A. Mokdad, A. Moran, K. Mulholland, M. N. Nair, L. Naldi, K. M. V. Narayan, K. Nasseri, P. Norman, M. O'Donnell, S. B. Omer, K. Ortblad, R. Osborne, D. Ozgediz, B. Pahari, J. D. Pandian, A. P. Rivero, R. P. Padilla, F. Perez-Ruiz, N. Perico, D. Phillips, K. Pierce, C. A. Pope, E. Porrini, F. Pourmalek, M. Raju, D. Ranganathan, J. T. Rehm, D. B. Rein, G. Remuzzi, F. P. Rivara, T. Roberts, F. R. De León, L. C. Rosenfeld, L. Rushton, R. L. Sacco, J. A. Salomon, U. Sampson, E. Sanman, D. C. Schwebel, M. Segui-Gomez, D. S. Shepard, D. Singh, J. Singleton, K. Sliwa, E. Smith, A. Steer, J. A. Taylor, B. Thomas, I. M. Tleyjeh, J. A. Towbin, T. Truelsen, E. A. Undurraga, N. Venketasubramanian, L. Vijayakumar, T. Vos, G. R. Wagner, M. Wang, W. Wang, K. Watt, M. A. Weinstock, R. Weintraub, J. D. Wilkinson, A. D. Woolf, S. Wulf, P.-H. Yeh, P. Yip, A. Zabetian, Z.-J. Zheng, A. D. Lopez and C. J. Murray, *Lancet* **2012**, *380*, 2095–2128.

[41] T. J. Ruckwardt, C. Luongo, A. M. W. Malloy, J. Liu, M. Chen, P. L. Collins, B. S. Graham, *J. Immunol.* **2010**, *185*, 4673–4680.

[42] P. Billam, K. L. Bonaparte, J. Liu, T. J. Ruckwardt, M. Chen, A. B. Ryder, R. Wang, P. Dash, P. G. Thomas, B. S. Graham, *J. Biol. Chem.* **2011**, *286*, 4829–4841.

[43] M. A. Lemes, A. Pialat, S. N. Steinmann, I. Korobkov, C. Michel, M. Murugesu, *Polyhedron* **2016**, *108*, 163–168.

[44] A. M. F. van der Gracht, M. A. R. de Geus, M. G. M. Camps, T. J. Ruckwardt, A. J. C. Sarris, J. Bremmers, E. Maurits, J. B. Pawlak, M. M. Posthoorn, K. M. Bonger, D. V. Filippov, H. S. Overkleeft, M. S. Robillard, F. Ossendorp, S. I. van Kasteren, *ACS Chem. Biol.* **2018**, *13*, 1569–1576.

[45] J. J. Neefjes, L. Smit, M. Gehrmann, H. L. Ploegh, *Eur. J. Immunol.* **1992**, *22*, 1609–1614.

[46] A. Porgador, J. W. Yewdell, Y. Deng, J. R. Bennink, R. N. Germain, *Immunity* **1997**, *6*, 715–726.

[47] J. Karttunen, N. Shastri, *Proc. Natl. Acad. Sci.* **1991**, *88*, 3972–3976.

[48] Z. Shen, G. Reznikoff, G. Dranoff, K. L. Rock, *J. Immunol.* **1997**, *158*, 2723–30.

[49] N. K. Devaraj, G. M. Thurber, E. J. Keliher, B. Marinelli, R. Weissleder, *Proc. Natl. Acad. Sci.* **2012**, *109*, 4762–4767.

[50] K. A. Hogquist, S. C. Jameson, W. R. Heath, J. L. Howard, M. J. Bevan, F. R. Carbone, *Cell* **1994**, *76*, 17–27.

[51] A. B. Lyons, C. R. Parish, *Determination of Lymphocyte Division by Flow Cytometry*, **1994**.

[52] M. Huse, *Immunology* **2010**, *130*, 151–157.

[53] M. Royzen, G. P. A. Yap, J. M. Fox, *J. Am. Chem. Soc.* **2008**, *130*, 3760–3761.

[54] J. A. Neal, D. Mozhdehi, Z. Guan, *J. Am. Chem. Soc.* **2015**, *137*, 4846–4850.